Joint Biotechnology Master Program

Palestine Polytechnic University
Deanship of Graduate Studies and Scientific Research

Bethlehem University
Faculty of Science

Mutations in *SNX10* and *TCIRG1* genes implicate the pathogenicity of Malignant infantile osteopetrosis in Palestine

By

Grace Nabil Rabi`

In Partial Fulfillment of the Requirements for the Degree

Master of Biotechnology

Spring, 2019

The undersigned hereby certify that they have read and recommend to the Faculty of Scientific Research and Higher Studies at the Palestine Polytechnic University and the Faculty of Science at Bethlehem University for acceptance a thesis entitled:

"Mutations in *SNX10* and *TCIRG1* genes implicate the pathogenicity of Malignant infantile osteopetrosis in Palestine"

by

Grace Nabil Rabi`

A thesis submitted in partial fulfillment of the requirements for the degree of Master of Science in biotechnology.

Graduate Advisory Committee:

Committee Member(Student's Supervisor)	Date
Prof. Dr. Moien Kanaan – Bethlehem University	
Committee Member (Internal Examiner)	Date
Prof. Dr. Mazin Qumsiyeh – Bethlehem University	
Committee Member (External Examiner)	Date
Dr. Mahmoud Srour – Birzeit University	

Approved for the Faculties

Dean of Graduate Studies and Scientific Research	Dean of Faculty of Science
Palestine Polytechnic University	Bethlehem University
Date	Date

"Mutations in *SNX10* and *TCIRG1* genes implicate the pathogenicity of Malignant infantile osteopetrosis in Palestine"

by Grace Nabil Rabi`

ABSTRACT

Autosomal recessive osteopetrosis (ARO) is a life-threatening rare disorder, attributed to reduced bone resorption by osteoclasts which results in increased bone density. Osteoclast dysfunction are mainly due to defined failure to maintain an acid pH at the ruffled border. Osteopetrosis is a genetically heterogeneous disorder but over 50% of humans with osteopetrosis have mutations in the transmembrane channels at the osteoclast ruffled border, especially in the V-ATPase proton pump. In this work, we identify the genetic basis of eight consanguineous Palestinian families of ARO, from Hebron and Ramallah cities. Most of these families are related with multiple affected members with early onset disease manifestations. Whole Exome Sequencing (WES) and microsatellite analysis were carried out. WES was verified by Sanger sequencing and identified two pathogenic variants in two different genes. In seven families, a missense mutation (p.R51Q) in a conserved amino acid of SNX10 co-segregated with the phenotype. Microsatellite analysis was performed on the affected individuals to show that (p.R51Q) mutation originated from the same ancestry. In only one family from Ramallah, a homozygous non-frameshift variant in *TCIRG1* (p.N462del) was identified, which is considered a novel mutation. It is speculated that mutations in both *SNX10* and *TCIRG1* result in V-ATPase deficiency weather directly or indirectly, leading to osteoclast defect. These results confirm the involvement of the *SNX10* gene in osteoclast physiology, and underlining the fact that partial deletions are part of the genotypic spectrum of *TCIRG1* mutations.

" الطفرات في جينات *SNX10* و *TCIRG1* تتسبب في الإصابة بمرض تصخر العظام الخبيث في فلسطين"

غريس نبيل ربيع

ملخص

مرض تصخر العظم الوراثي المتنحي (ARO) هو اضطراب نادر يهدد الحياة، ويعزى إلى انخفاض الارتشاف العظمي عن طريق هادمات العظم أو ما يعرف بخلايا الأوستيوكلاست مما يؤدي إلى زيادة كثافة العظام. ضعف خلايا الأوستيوكلاست يرجع أساسا إلى الفشل في الحفاظ على تركيز حمضي في الحواف المتعرجة (Ruffled Border) لهذه الخلايا. يعزى السبب وراء مرض تصخر العظم إلى العديد من العوامل أو الجينات الوراثية، ولكن؛ أكثر من 50 ٪ من البشر الذين يعانون من تصخر العظام لديهم طفرات في قنوات الغشاء المتواجدة على الحواف المتعرجة لخلايا الأوستيوكلاست، وخاصة في مضخة البروتون (V-ATPase). في هذه الدراسة، قمنا بتحديد الأساس الجيني لمرض التصخر العظمي في ثمانية عائلات فلسطينية معروفة بزواج الأقارب، من مدينتي الخليل ورام الله. تجمع معظم هذه العائلات درجة من القرابة، ويكون لدى العديد منهم أكثر من حالة إصابة بالمرض وتظهر الأعراض في سن مبكرة. في هذا العمل تم استخدام تقنية Whole-Exome Sequencing وأيضاً تم إجراء فحص Microsatellite Analysis. كشفت تقنية Whole-Exome Sequencing عن طفرتين ممرضتين في اثنين من الجينات المختلفة، وتم التحقق من ذلك عن طريق عمل Sanger Sequencing. في سبعة من العائلات المدروسة، تم الكشف عن طفرة تؤدي إلى تغير الحمض الأميني Arginine إلى الحمض الأميني Glutamine (p.R51Q) في جين *SNX10*. كما تم إجراء فحص Microsatellite Analysis على المصابين من هذه العائلات لإثبات أن هذه الطفرة نشأت من نفس الأصل أو السلالة. في عائلة واحدة من رام الله، تم الكشف عن الطفرة (p.N462del) في جين يسمى *TCIRG1*. ويتكهن أن الطفرات في كل من الجينات *SNX10* و *TCIRG1* تؤدي إلى فقدان مضخة البروتون-V) ATPase)بشكل مباشر أو غير مباشر، مما يؤدي إلى خلل في عمل خلايا الأوستيوكلاست. هذه النتائج تؤكد على أهمية دور جين *SNX10* في فسيولوجية خلايا الأوستيوكلاست، وتؤكد أن طفرات الحذف هي جزء من الطفرات الموجودة في جين *TCIRG1*.

DECLARATION

I declare that the Master Thesis entitled "dissertation title" is my own original work, and hereby certify that unless stated, all work contained within this thesis is my own independent research and has not been submitted for the award of any other degree at any institution, except where due acknowledgment is made in the text.

Name and signature: _____Grace Nabil Rabi`_____

Date: _____

STATEMENT OF PERMISSION TO USE

In presenting this thesis in partial fulfillment of the requirements for the joint master degree in biotechnology at Palestine Polytechnic University and Bethlehem University, I agree that the library shall make it available to borrowers under rules of the library. Brief quotations from this thesis are allowable without special permission, provided that accurate acknowledgement of the source is made.

Permission for extensive quotation from, reproduction, or publication of this thesis may be granted by my main supervisor, or in [his/her] absence, by the Dean of Higher Studies when, in the opinion of either, the proposed use of the material is for scholarly purposes. Any copying or use of the material in this thesis for financial gain shall not be allowed without my written permission.

Name and signature: _____Grace Nabil Rabi`_____

Date: _____

Acknowledgments

I express my sincere appreciation to those who have contributed to this thesis and supported me in one way or the other during this amazing journey. Without them, this research work would not have been possible.

I would like to especially acknowledge Prof. Moien Kanaan for giving me the opportunity to join his laboratory and for his excellent guidance and encouragement. I would like to express my sincere gratitude to Hereditary Research laboratory family for giving me the opportunity to be a member of their team. Thank you for your enthusiastic vision of science, you really make me enjoy science. I would like to give special thanks to Amal Abu Rayyan and Christina Canavati for their wonderful teaching and wise advices that improve my work and knowledge. Also, thanks to Lara Kamal and Dr. Fouad Zahdeh for their help in the project which made this thesis possible. I would also like to thank Professor Dr. Mazin Qumsiyeh.

My acknowledgement would be incomplete without thanking the biggest source of my strength, my family. The blessings of my parents and the love and care of my brothers and sister, you have all made a tremendous contribution in helping me reach this stage in my life. I would like to dedicate this work to my mother whose dreams for me have resulted in this achievement and without her loving upbringing and nurturing; I would not have been where I am today and what I am today.

A heartfelt thanks to my supportive wonderful husband, I owe you a big thanks. The love and support that you gave has motivated me to work harder and to strive towards my goal.

Abbreviations

ACP5	Acid phosphatase 5, tartrate resistant (encodes TRAP)
ADCY6	Adenylate Cyclase 6
ADO	Autosomal dominant osteopetrosis
ARO	Infantile malignant autosomal recessive osteopetrosis
ATP	Adenosine triphosphate
BMT	Bone marrow transplantation
CAII	Carbonic anhydrase II
Cl-/HCO3-	Chloride/bicarbonate exchanger
ClCN7	Chloride channel 7 gene
CSF	Cerebrospinal fluid
DNA	Deoxyribonucleic acid
EDTA	Ethylenediaminetetraacetic acid
ERCC2	ERCC Excision Repair Cross-Complementing 2
EXAC	Exome Aggregation Consortium
FAM	Fluorescein amidite dye
HLA	Human leukocyte antigen
IARO	Intermediate autosomal recessive osteopetrosis
KRT82	Keratin 82
LRP5	Lipoprotein receptor-related protein 5
M-CSF	Macrophage colony stimulating factor
MITF	Microphthalmia-associated transcription factor

NTC	No template control
OPG	Osteoprotegerin
OSTM1	Osteopetrosis-associated transmembrane protein 1
PCR	Polymerase Chain Reaction
PMEL	Premelanosome Protein
POLYPHEN	Polymorphism Phenotyping
PLEKHM1	Pleckstrin homology domain containing family M (with RUN domain) member 1 deficiency
RANK	Receptor activator of nuclear factor nb
RANKL	Receptor activator of nuclear factor nb ligand
RBC	Red blood cells
SDS	Sodium Dodecyl Sulfate
SIFT	Scale-invariant feature transform
SNX10	Sorting nexin 10
STR	Short tandem repeat
TCIRG1	T-cell immune regulator 1 gene
TRAP	Tartrate resistant acid phosphatase
V-ATPase	Vacuolar type H+-ATPase
WBC	White blood cells
WES	Whole exome sequencing

List of Figures

List of Tables

Table of Contents

CHAPTER 1

1.0 Introduction

Bone is a complex dynamic tissue that together with cartilage forms the skeletal system. The skeleton provides mechanical support for the body and site of muscle attachment for locomotion as well as protection for vital organs (Clarke, 2008). Bone diseases in humans comprise both common and rarer conditions, and often have devastating consequences. Many skeletal diseases, such as osteoporosis, osteopetrosis, and rheumatoid arthritis are primarily caused by defects in osteoclasts, the sole bone-resorbing cells. Under physiological conditions, the osteoclast participates in ossification during longitudinal bone growth as well as in bone remodeling during adulthood (Long et al., 2013).

Bone is a living organ which is constantly degraded and rebuilt throughout life to maintain mineral homeostasis and repair damage; a process known as bone remodeling (Sims and Gooi, 2008). This process involves the resorption of old bone by osteoclasts, and the formation of new bone by the osteoblasts, all processes important for maintaining a healthy skeleton. During adulthood, about 10% of bone is replaced each year with complete renewal every 10 years (Seeman and Delmas, 2006). Bone resorption is initiated by attachment of osteoclasts to the surface of bone to be resorbed at specialized membrane domains called ruffled borders (Teitelbaum, 2000). In this resorption lacuna, local acidification leads to dissolution of mineral, and secretion of proteolytic enzymes completes degradation of the exposed collagen.

Under normal circumstances resorbed bone is always replenished with equal amounts of new bone in the healthy adult. However, hormonal changes or genetic defects can skew the balance and lead to pathological changes in bone. Hence, mutations affecting osteoclast and acidification process, result in defective bone resorption and leads to the severe hereditary autosomal recessive osteopetrosis (ARO) (Tolar et al., 2004). Osteoclasts with defective bone resorption will lead to disordered skeleton

architecture, as old bone is not broken down and bones become unusually dense. However, their increased density does not improve their strength, instead it results in brittle bones that are subjected to fractures with poor healing (Tolar et al., 2004).

The majority of humans with osteopetrosis have mutations in the transmembrane channels at osteoclast ruffled border, especially in the proteins or protein subunits of vacuolar type H+-ATPase (V-ATPase) proton pump (Taranta et al., 2003). The primary role of V-ATPases in osteoclasts is to acidify intracellular compartments and for extracellular acidification necessary for bone resorption. That's why mutations in the *TCIRG1* gene encoding for subunit A3 of the proton pump (V-ATPase) are responsible for more than one-half of ARO cases (Frattini et al., 2000). Another important channel is the chloride-proton antiporter ClCN-7 which acts in concert with the V-ATPase at the ruffled border by transporting chloride ions into the resorption area (Kornak et al., 2001). ClCN7 mutations are responsible for many cases of Recessive, and Dominant Osteopetrosis. Mutations in other genes are less common, and in about 30 percent of all cases of osteopetrosis, the cause of the condition is unknown.

The broad objective of this project is to systematically recruit familial cases of osteopetrosis across different regions in Palestine. The goals of this work were to identify the genetic basis of osteopetrosis in these families, to correlate the molecular presentation of the patients with their clinical picture, to increase awareness among consanguineous Palestinian families, and to consult these families for better future management and prognosis.

CHAPTER 2

2.0 Literature Review

In healthy bone, formation and resorption are in balance and tightly coupled, resulting in no net loss or gain of bone mass (Lazner et al., 1999). Altered coupling results in several pathological conditions. Excessive bone resorption caused by increased osteoclast activity leads to conditions such as osteoporosis (a low bone mass condition), whereas; impaired bone resorption caused by either reduced osteoclast activity or absence of osteoclasts leads to osteopetrosis (a high bone mass condition) (Lazner et al., 1999).

This literature review will provide background information about bones and the cells found within bones with a special emphasis on the osteoclast, osteoclast differentiation and function. After that, osteopetrosis classification will be discussed, and the rest of the chapter will focus on the most severe form of osteopetrosis, ARO. This will include; the clinical manifestation, treatment, and the genetic heterogeneity of ARO. Finally, ARO mutations affecting acidification process will be addressed with the focus on mutations resulting in V-ATPase deficiency whether directly or indirectly.

2.1 The Cellular Components of Bone

- **The osteoblast**

Osteoblasts are bone forming cells found at the bone surface. They are mainly responsible for synthesis of the organic matrix, the osteoid, and subsequently control mineralization of the matrix (Capulli et al., 2014). Moreover, an important function of osteoblasts is the regulation of osteoclast differentiation and resorption. Osteoblasts are derived from immature mesenchymal stem cells (Osteoprogenitor cells) (Capulli et al., 2014). Osteoprogenitor cells persist throughout postnatal life as bone-lining cells with the capacity to be reactivated in the adult during the repair of bone

fractures and other injuries. The terminal stages of osteoblast differentiation result in three fates for these cells: they may become inert or quiescent bone-lining cells, become trapped in their own secreted mineralized matrix forming osteocytes, or undergo apoptosis (Manolagas, 2000; Aubin, 2001; Capulli et al., 2014).

- **The osteocyte**

Osteoblasts differentiate into osteocytes after they are trapped within the mineralized matrix they produce (Manolagas, 2000). It has been suggested that 10-20% of osteoblasts differentiate into osteocytes. Osteocytes are connected to each other and to the bone surface to form an extensive network of small channels, called cannaliculi. Through this network osteocytes sense and respond to strain, receive nutrients and have direct communication with osteoblasts, osteoclasts and surface-lining cells (Manolagas, 2000). The general function of the osteocyte is thought to include mechanosensory activity actively directing the actions of osteoblasts and osteoclasts, in response to external physiological stress (Manolagas, 2000; Bonewald, 2011). In addition, Osteocyte apoptosis or necrosis may define the location where bone remodeling is needed (Bonewald, 2011; Sims and Vrahnas, 2014).

- **The osteoclast**

Osteoclasts are large multinucleated cells, found at the bone surface, responsible for bone resorption and mobilization of calcium. The osteoclasts originate from the hematopoietic stem cell population of the monocyte-macrophage lineage which present in the adjacent bone marrow (Baron, 1989). Non-resorbing osteoclasts are motile cells without distinct membrane domains. Only the mature active osteoclast is capable of resorption function as it’s a highly polarized cell, and have the expression of specialized membrane domains on the apical surface facing the bone.

- **Osteoclastogenesis**

Osteoclastogenesis is a well-characterized process consisting of three consecutive steps starting from precursors recruitment, their fusion into mature polynucleated osteoclasts and finally the activation of these mature osteoclasts (Lézot et al., 2015). The two major signaling factors implicated in these differentiation steps are presented in Figure 1. The transcription factors, PU.1 and MITF, acting early in the monocyte-macrophage lineage regulates the development of the hematopoietic precursor cells and the committed precursors to become osteoclasts (Shalhoub et al., 2000; Way et al., 2009). Generation of osteoclasts require physical contact of the precursor cells with specific mesenchymal cells such as osteoblasts or marrow stromal cells. It is now clear that macrophage colony stimulating factor (M-CSF) and receptor activator of nuclear factor- Kappa B ligand (RANKL), both expressed in osteoblast/stromal cells, are essential for osteoclastogenesis (Felix et al., 1990). This signaling pathway promotes proliferation of osteoclast precursor cells and survival of the differentiated osteoclast.

RANKL, a member of the TNF superfamily, is a membrane-residing protein on osteoblasts and their precursors that recognizes its receptor, RANK, on marrow macrophages, which triggers them to attain the osteoclast phenotype (Li et al., 2000; Zhao et al., 2007). RANKL activity is negatively regulated by osteoprotegerin (OPG), which competes with RANK as a soluble decoy receptor. OPG, like RANKL, is produced by osteoblast lineage cells (Simonet et al., 1997). The disturbance of the OPG/RANKL ratio seems to dictate the rate of bone resorption in a number of pathological states (Simonet et al., 1997).

The signaling downstream of RANK/RANKL is not fully understood. Committed osteoclast precursors will start to fuse to multinuclear osteoclasts (Yagi et al., 2005). As pre-osteoclasts fuse, they start expressing a range of proteins, such as tartrate resistant acid phosphatase (TRAP), cathepsin K, Chloride channel 7 (ClC-7), and the osteoclastic vacuoloar H+-ATPase (V-ATPase),

including its subunit T-cell immune regulator 1 (TCIRG1)(also referred to as the a3 subunit), which are important for correct osteoclast resorptive function (Kornak et al., 2000).

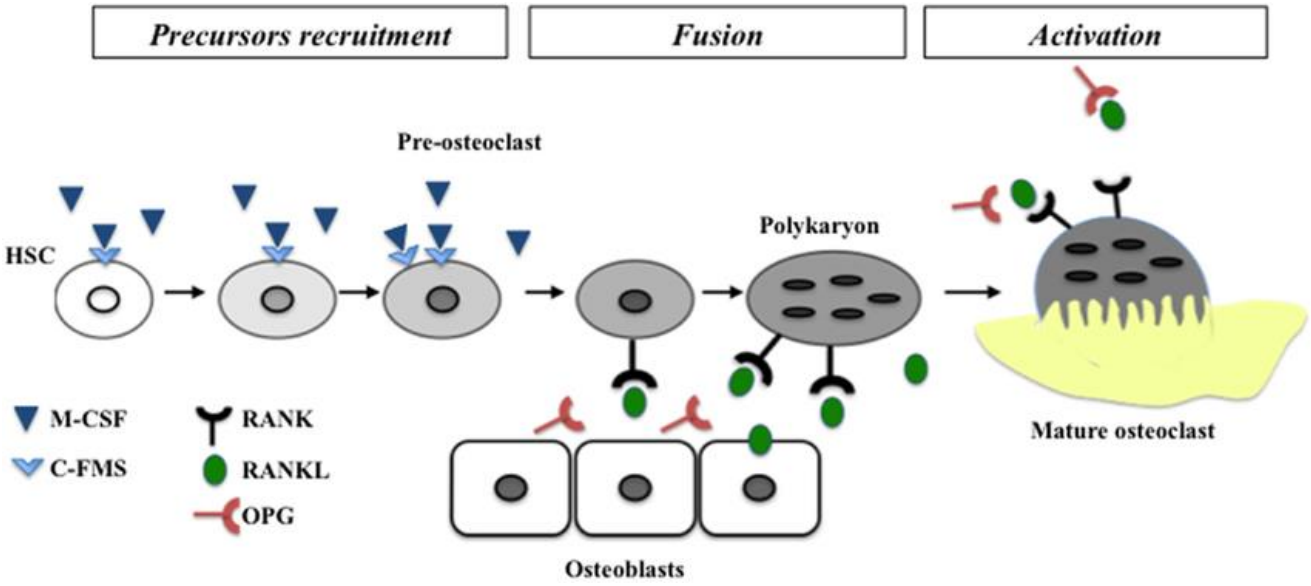

Figure 1: Important steps in osteoclast differentiation (Lézot et al., 2015).

- **Polarization of resorbing osteoclasts**

When bone resorption is initiated osteoclasts attach to distinct sites on the bone matrix, become polarized and create three specialized membrane domains (Figure 2); a sealing zone on the apical side, which is the extracellular adhesion structure, and a ruffled border where the actual degradation of bone takes place as well as a functional secretory domain on the basolateral surface (Vaananen and Horton, 1995).

Simultaneously, the cytoskeleton undergoes extensive re-organization. At the sealing zone, actin cytoskeleton forms an attachment ring. The sealing zone isolates the resorption lacuna from the extracellular fluid, thus creating a compartment at the site of the ruffled border where the decalcification and degradation of the matrix occurs (Zou et al., 2007). The functional secretory domain is located at the center of the basolateral membrane and is in contact with the extracellular fluid, capillaries and also other cells.

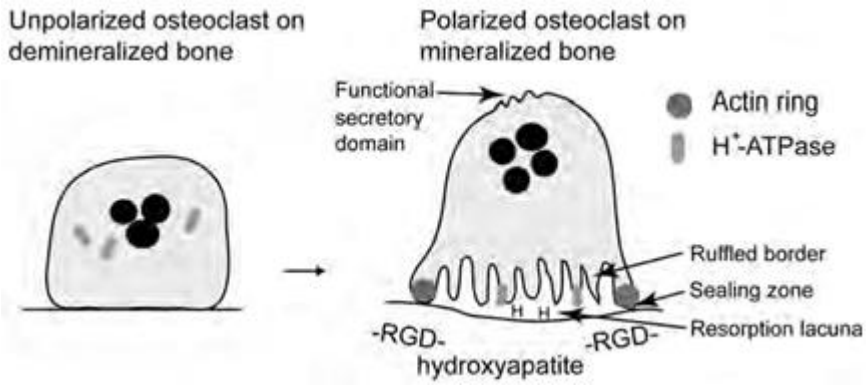

Figure 2: Unpolarized and polarized osteoclast.

- **The Ruffled Border**

In resorbing osteoclasts, the ruffled border forms a villous-like structure penetrating into the bone matrix, demarcated by the sealing zone (Figure 3). The ruffled border is formed by fusion of acidic intracellular vesicles containing a vacuolar-type H+-ATPase (V-ATPase), which pump hydrogen ions into the resorption lacuna (Boyle et al., 2003; Teitelbaum, 2007). The protons are generated in the cytoplasm by Carbonic anhydrase II (CAII). The alkalinization of the cytoplasm induced by the massive outward proton transport is balanced by an electroneutral chloride/bicarbonate exchanger. The Cl- that enters the cell in exchange for HCO3-, is transported into the resorptive lacuna via a chloride channel, charge-coupled to the V-ATPase, thus generating HCl, which generate an ambient pH ~4.5 in the resorption lacuna. The acid secreted into the resorption lacuna has two functions. (Kornak et al., 2001; Li et al., 1999; Marks, Jr. et al., 1985). Firstly, it mobilizes the mineral phase exposing the organic matrix of bone for degrading proteases, and secondly provides the acidic pH that is required for the action of lysosomal cysteine proteinases (Taranta et al., 2003; Waguespack et al., 2007).

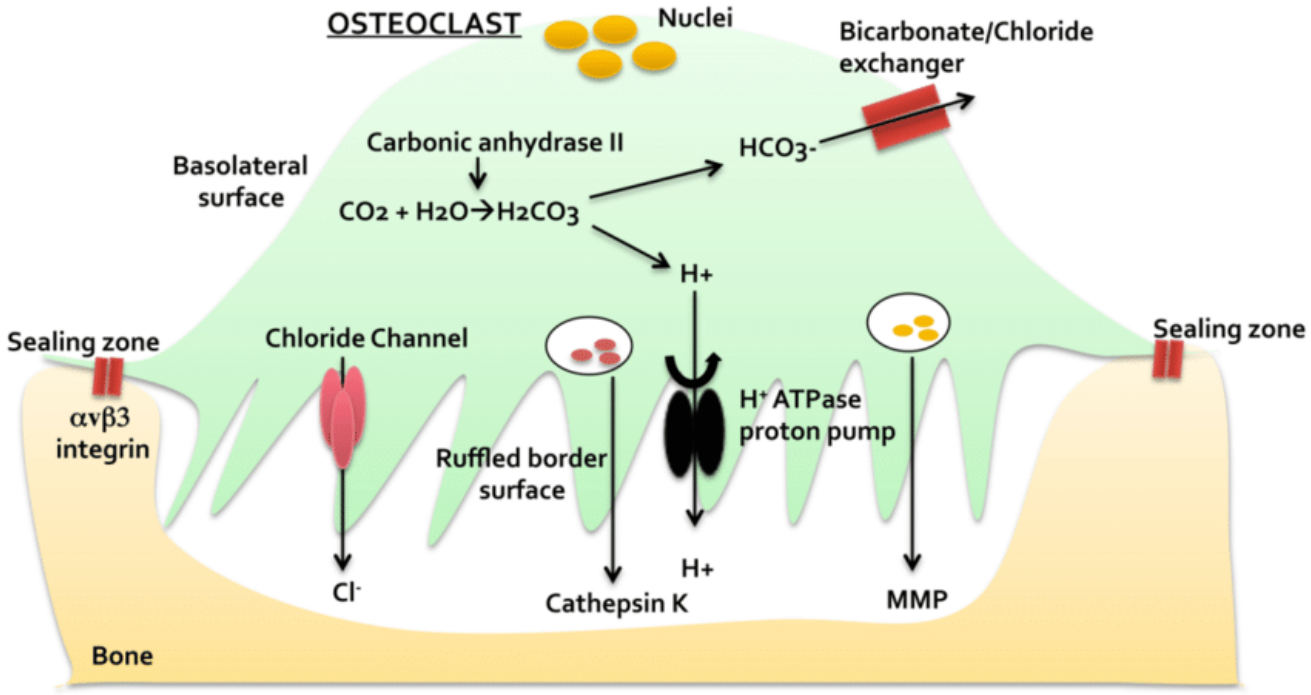

Figure 3: Resorptive mechanisms of an osteoclast (Dole et al., 2015).

2.2. Osteopetrosis Classification

Osteopetrosis is, per definition, increased bone mass due to arrested bone resorption, reflecting either failed normal recruitment of osteoclasts or resorptive dysfunction of the differentiated cells (Bollerslev et al., 1993; Balemans et al., 2005). Osteopetrosis is a heterogenous group of rare genetic diseases, grouped by severity of the disease based on histomorphometric and clinical parameters into a milder adult form, an intermediate form and a fatal infantile malignant form (Del Fattore et al., 2006; de Vernejoul and Benichou, 2001). Table 1 contains a summary of the genetic mutations in essential osteoclast genes that result in an osteopetrotic phenotype (Del Fattore et al., 2008; Tolar et al., 2004).

2.2.1. Autosomal Dominant Osteopetrosis

The mildest form of osteopetrosis is called autosomal dominant osteopetrosis (ADO). This form is further subdivided into two groups, ADOI, caused by overactive osteoblasts and ADOII,

caused by underactive osteoclasts. ADOI is characterized by high bone mass with increased mineralizing surface caused by a combination of overactive osteoblasts and low numbers of small osteoclasts and results from gain of function mutations such as mutations in the low-density lipoprotein receptor-related protein 5 (LRP5) gene, which alters the osteoblast's ability to support osteoclastogenesis (Henriksen et al, 2005). The most common type of osteopetrosis is ADOII, also known as Albers-Schonberg disease. ADOII is caused by mutations in the CLCN7 gene that are primarily missense mutations of conserved amino acids and results in inactive osteoclasts (Cleiren et al., 2001).

2.2.2. Intermediate Autosomal Recessive Osteopetrosis

Intermediate autosomal recessive osteopetrosis (IARO) is intermediate in severity in that it is more clinically severe than dominant forms and less severe than the infantile malignant form. IARO is caused by certain mutations to ClCN7 and CAII genes (Margolis et al., 2008).

2.2.3. Infantile Malignant Autosomal Recessive Osteopetrosis

The infantile malignant form of osteopetrosis (ARO) is the most severe form (Balemans et al., 2005). It results in dense brittle bone with severely reduced marrow spaces, leading to anemia and thrombocytopenia and compensatory hepatosplenomegaly. Most children with ARO die within 4 years of birth often from infections unless early intervention by the only known treatment which is bone marrow transplant. The most common genetic mutations that cause ARO are in the T-cell immune regulator 1 (TCIRG1) gene, which codes for the a3 subunit of V-ATPases (Kornak et al., 2000; Frattini et al., 2000). And from now on, the focus of this thesis will be on this type of osteopetrosis, the ARO form.

Table 1. Osteoclast Features Resulting from Genetic Mutations that Cause Osteopetrosis

Protein (Gene)	Function	Osteoclast Features	Disease	Reference
TCIRG1/a3 (*TCIRG1*)	Acidification of resorption lacuna	Increased osteoclast number, not polarized, no RB, no function	ARO	(Kornak et al., 2000; Frattini et al., 2000)
CLC-7 *(CLCN7)*	Acidification of resorption lacuna	Increased osteoclast number, enlarged under developed RB, no function	ARO/ADO	(Kornak et al., 2001; Frattini et al., 2003; Cleiren et al., 2001; Campos-Xavier et al., 2003)
OSTM1 *(OSTM1)*	Acidification of resorption lacuna	Increased osteoclast number, immature RB, no function	ARO	(Chalhoub et al., 2003; Pangrazio et al., 2006)
SNX10 *(SNX10)*	Endosomal/vesicular trafficking	Decreased osteoclasts number, bone resorptive capacity is impaired	ARO	(Pangrazio et al.,2013)
RANKL (*TNFSF11A)*	Osteoclastogenesis	No osteoclasts, decreased bone formation	ARO	(Guerrini et al., 2008; Pangrazio et al., 2012)
PLEKHMI (PLEKHMI)	Vesicular trafficking	Normal osteoclast number, bone resorptive capacity is impaired.	IARO	(Pettit et al., 2001; Guerrini et al., 2008)
CAII *(CAII)*	Acidification of resorption lacuna	Increased osteoclasts number, decreased function	IARO	(Margolis et al., 2008)
TRAP(ACP5)	Acidification of resorption lacuna	Increased osteoclast number, not polarized, reduced function	None identified	(Hollberg et al., 2002)

2.3. Malignant Infantile ARO: The Most Severe Form

2.3.1. Clinical Manifestations

ARO which is the most severe type of osteopetrosis can lead to death in the first decade of life if left untreated. Symptoms vary depending on the exact gene mutation. Affected individuals usually have growth retardation, delayed psychomotor development, delayed tooth development, micrognathia, osteosclerosis, and osteomyelitis (Cummings and Proia, 2004; Herman and Siegel, 2007). In addition, craniofacial bone abnormalities can result in hydrocephalus, nasal obstruction and nerve compression that lead to progressive blindness and deafness (Balemans et al., 2005). Patients can also present with seizures due to low levels of calcium in the blood. The most severe complication of ARO is bone marrow suppression (Balemans et al., 2005). Medullary haematopoiesis is inhibited due to the abnormal expansion of bone, resulting in secondary expansion of extramedullary haematopoiesis sites such as the liver and spleen. This may lead to life-threatening pancytopaenia, and susceptible frequent infections such as pneumonia and urinary tract infections.

2.3.2. Current Treatment

While mild forms of osteopetrosis can go undetected for many years, ARO is a fatal disease and without hematopoietic stem cell transplantation the disease is lethal before the age of 6 years. Bone Marrow transplantations (BMT) have been applied in a number of patients and the long-term clinical outcome is highly dependent on human leukocyte antigen (HLA) matching, and the age of the patient at transplantation (Sobacchi et al., 2013). Studies have shown that transplantations performed before the age of 10 months increase the chance of full engraftment, while transplantations performed at older age increase the risk of graft rejection

or autologous reconstitution (Sobacchi et al., 2013). Overall, BM transplantation is an effective therapy for treatment of osteopetrosis if initiated early. However, in cases where no HLA matched donors can be found, there is a clear need for alternative treatment options, such as gene therapy, however; this treatment option is outside the scope of this thesis and will not be discussed further.

2.4. Genetic Heterogeneity of ARO

Most cases of ARO are caused by defects in gene products involved in the acidification of resorption lacuna, whether in the acidification machinery itself or during vesicular trafficking and transport (Popoff and Marks, 1995). Acid secretion is dependent on two key molecules, which facilitate proton transport: the proton pump vacuolar ATPase (V-ATPase) and the chloride-specific ion channel, chloride channel 7 (CLCN-7) (Kornak et al., 2001). Homozygous mutations in the genes encoding the a3 subunit of V-ATPase (*TCIRG1*) and the CLCN-7 produce severe malignant osteopetrosis phenotypes. *TCIRG1* mutations are responsible for autosomal recessive osteopetrosis in more than 50% of affected individuals (Sobacchi et al., 2001) underscoring the crucial role of V-ATPase in osteoclast function. Since vesicular trafficking is essential for osteoclast formation and activity, Sorting nexin 10 (*SNX10*) gene has been identified as a new osteopetrosis associated gene in consanguineous families of Palestinian origin (Aker et al., 2012). Therefore, this chapter will focus on both *TCIRG1* and *SNX10* genes mutations which encompass the most frequent genetic changes of ARO in the Palestinian population.

2.4.1. Role of V-ATPase Proton Pump in Osteopetrosis

2.4.1.1. V-ATPase Structure

V-ATPases has two domains, the cytosolic V1 domain and the transmembrane Vo domain,

which are composed of at least 14 subunits as shown in Figure 4 (Jefferies et al., 2008; Stevens and Forgac, 1997). The domains are connected by a central stalk composed of the D and F subunits and by three peripheral stalks formed by the C, E, G and H subunits. The V1 contains eight subunits (A-H) and includes the sites where ATP is hydrolyzed (subunits A and B) (Jefferies et al., 2008). The membrane-embedded Vo domain, where proton translocation occurs, includes subunits a, c, c", d, e and the accessory subunits Ac45 and M8-9 (Stevens and Forgac, 1997).

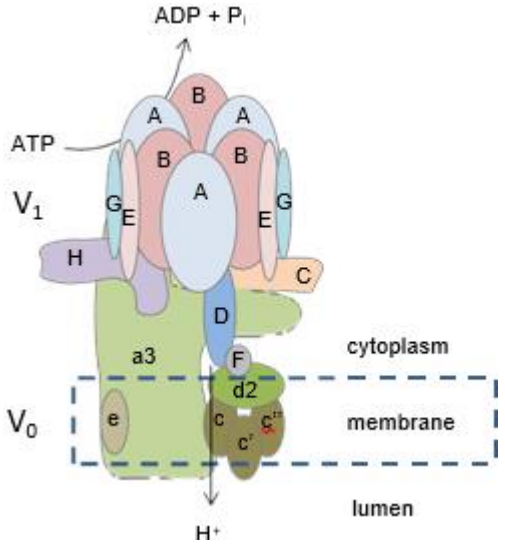

Figure 4: Structural overview of the osteoclastic V-ATPase (Jefferies et al., 2008).

2.4.1.2. *TCIRG1* Gene and its Role in ARO

*TCIRG1*gene encodes the a3 subunit of vacuolar H(+)-ATPase. And mutations in *TCIRG1* (OMIM: 604592) account for the majority of cases of osteopetrosis (Frattini et al., 2000). T Cell Immune Regulator 1 (*TCIRG1*) is located on chromosome 11q13.2, molecular location: chr11:68,038,994-68,053,845 (UCSC Genome Browser assembly ID: hg38). *TCIRG1* contains 20 exons, and through alternate splicing in exon 7 gives rise to two isoforms: TCIRG1-isoa and TCIRG1-isob (Frattini et al., 2000). TCIRG1-iso-a is a full-length isoform and encodes a3

subunit of vacuolar H+-ATPase. TCIRG1-iso-b is a shorter isoform, lacking the first 5 exons of the longer isoform, it plays an essential role in immune response (Makaryan et al., 2014).

The 'a' subunit of the V-ATPase is notable for having a C-terminal portion that participates in proton translocation (Kornak et al., 2000). There are 4 isoforms of 'a' subunit which are (a1, a2, a3, and a4), but the a3 isoform encoded by *TCIRG1* gene is the one that is expressed in osteoclasts (Toyomura et al., 2000). Therefore, mutations in *TCIRG1* will prevent the targeting of the V-ATPase to the plasma membrane of osteoclasts, and leads to V-ATPase deficiency.

2.4.2. *SNX10* Gene and its Role in ARO

In *Homo sapiens*, homozygosity for mutations in Sorting nexin 10 (*SNX10*) gene has been reported to cause Autosomal Recessive Osteopetrosis ARO (Pangrazio et al., 2013). *SNX10* (OMIM: 614780) is located on chromosome 7p15.2, molecular location: chr7: 26,291,894-26,374,329 (UCSC Genome Browser assembly ID: hg38). *SNX10* belongs to a large group of 33 proteins of the sorting nexin family. Members of this family share an N-terminal (PX) domain, which is a phosphoinositide binding domain. This domain is involved in intracellular processes such as endocytosis, and vesicle-mediated protein trafficking (Chen et al., 2012). The *SNX10* gene has six exons that encode 224 amino acids by which the 38–135 residues constitute the PX domain. Mutations in the PX domain of *SNX10* interfere with their endosomal pathway (Yao et al., 2009).

Several hypotheses have been proposed to illustrate the role of *SNX10* in osteopetrosis. But the most acceptable hypothesis suggests that *SNX10* is responsible for the vesicular trafficking of the V-ATPase complex from the Golgi network or for its targeting to the ruffled border of osteoclasts (Chen et al., 2012). V-ATPase as previously mentioned pumps protons at the

osteoclast-bone interface. Thus, a mutation in *SNX10* would therefore result in an indirect or secondary V-ATPase deficiency, therefore the inability to acidify the resorption lacuna. It was later shown that *SNX10* interacts with the V-ATPase D subunit (Sun-Wada et al., 2015) and recruits the proton pump complex to the ruffled border.

CHAPTER 3

3.1. Problem Statements and Objectives

A very serious problem among the Palestinian population is consanguineous marriage, which increases recessive genetic disorders (Zlotogora, 1997). Recent advances in molecular genetics have enabled us to minimize the effect of the genetic diseases and thus are critical in public health from diagnostic to prognostic to prediction. Recent molecular high-throughput technologies have enabled researchers to investigate conditions that were challenging to study before (Blazer and Hernandez, 2006). These include candidate gene sequencing, linkage, microsatellite analysis, SNP array technologies, and whole exome sequencing.

In this study, 9 Palestinian families from Al-Karma and Yatta Hebron villages, and one family from Shibteen village in the west of Ramallah were investigated to identify the causative mutation for osteopetrosis phenotype in the affected individuals of these families. Most family members have high degree of relatedness especially those from the Karma village, thus they have similar phenotype presentation, and more or less the same disease age onset. Having this in mind, we speculated that these families might have the same region of shared homozygosity, thus the same gene mutation in almost most of the affected individuals, which may facilitate disease gene identification approach.

The main goal of this study was to identify the causative mutations of osteopetrosis in the 10 Palestinian families and to deduce their developmental consequences. More specifically the study aims to screen genes previously associated with osteopetrosis, to identify candidate mutation/s using WES and bioinformatics tools, to confirm the mutation/s by checking segregation of the variant/s with osteopetrosis phenotype in all family members, to relate the

molecular presentation of the probands to their clinical picture, and to provide consultancy to affected families regarding consanguineous marriages.

3.2. High-throughput Technologies

3.2.1. Haplotype Analysis

Microsatellite markers or known as short tandem repeat (STR) markers, are noncoding polymorphic repetitive DNA sequences, found interspersed in the genome (Marín-García, 2011). Microsatellites are useful because of their high degree of variability and reproducibility. Microsatellite analysis depends on the separation of fluorescently labeled fragments using capillary electrophoresis and determination of the relative size of the fragments (Young et al, 2010). Microsatellite genotyping is a widely accepted tool for Forensic DNA testing, linkage analysis, association studies, individual relatedness testing, and gene disease identification. In linkage studies, a large number of families can be examined to see when the alleles of specific markers are inherited together with a certain phenotype or disease. In a genome screen, markers must not be very far from the underlying genetic cause of the disease than the detectable level of marker (Froeschke et al., 2014). GeneScan Analysis Software can be used to analyze DNA fragments as a function of fragment size or migration time. By which the genescan results are displayed as peaks profile, each peak represents a certain PCR fragment size (MCDONALD et al., 1997). Accurate size can be obtained by comparing the fragments size by a Rox -labeled internal size calibrator.

3.2.2. Whole-Exome Sequencing

Whole exome sequencing is an approach that belongs to the next generation sequencing technology and has been developed to study the approximately 1% of the human genome, by

capturing only exonic regions. As the majority of genetic variants that underlie Mendelian disorders disrupt protein-coding sequences, this approach has become a standard practice in clinical genetics for investigating the basis of human diseases (Yang et al., 2013). Whole exome sequencing workflow consists of four basic steps including; library preparation, cluster generation, sequencing, and data analysis. Library preparation includes genomic DNA quantitation, fragmentation and adaptor ligation, followed by PCR amplification. Libraries are then hybridized to exon-specific biotinylated probes, then fragments are enriched with capture beads. Fragments are finally amplified, producing sequence-ready targets. Sequences are then aligned to a reference genome for variant detection. This approach has been a powerful in identification of causal genetic variants in many different diseases.

CHAPTER 4

Materials and Methods

4.1. Recruitment of Study Subjects

Orthopedist, pediatricians and other health care professionals from Hebron were contacted to refer families with infantile osteopetrosis to Hereditary Research Laboratory at Bethlehem University for further clinical examination and genetic analysis. Participating families were asked to sign an informed consent to state their voluntary agreement to participate in the research study, after they were informed of the purpose and procedures of the study. Ten Palestinian families were recruited, 8 families from Al-Karma, Hebron village, one family from Yatta, Hebron village, and one family from Shibteen village in the west of Ramallah. Blood samples were collected from all family members, the parents, affected individuals, and their healthy siblings. Osteopetrosis diagnosis was confirmed for the affected individuals after referring to their medical records including X-ray and radiography reports, Clinical and hematological tests, and hearing and vision examinations. Bone marrow transplantation reports were reviewed to see if the surgery was performed, and the date of surgery and its success rate. Questionnaires comprising a diagnostic interview and a family composition form including family pedigree were administered.

4.2. DNA Extraction from Blood by Salting-out Method

Around 5 ml of peripheral blood was withdrawn from each participant and transferred to a sterile EDTA vacutainer tube. The blood was then transferred into a 50 ml centrifuge tube, and a 45 ml of RBC lysis buffer (155 mM NH4CL, 100 M NH4HCO3, 0.1 mM EDTA) was then added to each tube to lyse the red blood cells. The tubes were kept on ice for approximately 20 minutes

then centrifuged at 2000 rounds per minute (rpm) for 10 min at 4^{o}C. The supernatant was carefully discarded then the pellet was resuspended with 15 ml of RBC lysis buffer and centrifugation was repeated using the same conditions. The white pellet was resuspended in 3 ml of WBC lysis buffer (50 mM Tris HCL pH = 7.5, 100 mM NaCl, 1 mM EDTA), 100 µl of 20% sodium dodecyl sulfate SDS (Amresco, Cat# 1328-M112) and 100 µl of 5mg/ml Proteinase K (Amresco, Cat# E195). The tubes were then incubated overnight at 37 ^{o}C in the incubator shaker. After incubation, 1 ml of 6M NaCl was added to each tube and was vigorously vortexed until the solution became foamy. The tubes were then centrifuged at 3000 rpm for 20 min at 25 ^{o}C and the supernatant was then poured into a 15 ml conical tube. The tubes were centrifuged again at the same conditions and the supernatant was poured in another 15 ml tube, avoiding the salt protein deposit. About 8 ml of 100% absolute cold ethanol was added to each tube containing the clear supernatant. The tube was then gently inverted until the DNA precipitated and was visible as thin white fibers. Fishing of DNA threads were done using Pasteur pipettes and was then washed in 70% ethanol and was let dry for 3-5 min. After air-drying, the DNA was finally transferred to a screw-capped tube containing an appropriate volume (depending of the amount of DNA) of 0.02% sodium azide (Sigma Aldrich, Cat# S2002) to dissolve and preserve DNA, and prevent microbial growth.

4.3. Mutational Analysis and Genotyping

4.3.1. Primer Design

All primers were designed using Primer3 Input (version 4.0.0) software (http://primer3.ut.ee). 5' to 3' direction primer sequences, used in this thesis, are all listed in Appendix I, Table 7.

4.3.2. Polymerase Chain Reaction

The PCR reaction mixture include DNA polymerase enzyme, DNA template, forward and reverse primers, dNTPs, MgCl2 buffer, and sterile water. To prepare a 25µl PCR reaction, 12.5µl of PCR Ready Mix (Abgene, Cat# AB-0575-DC-LD) which contains *Taq* DNA polymerase, dNTPs (dATP, dCTP, dGTP and dTTP), MgCl2 and buffer was mixed with 10.5µl sterile, nuclease-free water and 0.5µl from each of the forward and the reverse primers. A master mix containing all PCR reagents, except the DNA template, was prepared to be sufficient for the number of planned reactions, by multiplying each volume of the used reagents by the number of samples. One extra reaction was added within each premix to serve as a no template control (NTC). 24µl of the master mix were then aliquoted in each reaction well, followed by the addition of 1.0µl of the DNA template (100 ng).

All PCR reactions were carried out in the Applied Biosystems Veriti™ 96-Well Thermal Cycler using touchdown PCR program for increased specificity and sensitivity in PCR amplification, the following table (Table 2) clarify the basic touchdown 60^{o}C program used in all PCR reactions of this thesis:

Table 2. Basic Touchdown 60°C PCR program

# of Cycles	Denaturation	Annealing	Extension
Step one: The initial denaturation			
1	95°C for 5 min		
Step two: Several cycles where the annealing temperature is gradually reduced			
3	95°C for 30 sec	68°C for 30 sec	72°C for 30 sec
3	95°C for 30 sec	66°C for 30 sec	72°C for 30 sec
3	95°C for 30 sec	64°C for 30 sec	72°C for 30 sec
3	95°C for 30 sec	62°C for 30 sec	72°C for 30 sec
35	95°C for 30 sec	60°C for 30 sec	72°C for 30 sec
Step three: The final extension			
1			72°C for 5 min
Step four: Hold			
∞			4°C for ∞

4.3.3. Gel Electrophoresis of Amplified PCR Products

To analyze PCR products on Gel Electrophoresis a 1.5% agarose gel was prepared by mixing 1.5 grams of agarose powder (SeaKem LE Agarose, Cat# 50004) with 100 ml 1X TAE buffer (2 M Tris pH= 8, 1 M acetic acid, 0.05 M EDTA pH = 8) in a microwavable flask. After 2-3 min in the microwave, the agarose was completely dissolved and few drops of ethidium bromide (Amresco, Cat# E406-5ML) were added to visualize the DNA upon UV exposure. Then the

solution was allowed to cool for few minutes on room temperature and poured into a gel caster after a comb was placed. After that the agarose gel was allowed to solidify for 10-15 minutes.

3µl of each PCR product were loaded into the wells of the gel along with an appropriate size marker, usually 100 bp DNA ladder (GeneRuler, Thermo Scientific, Cat# SM0241). After loading the samples, electrophoresis was performed in 1X TAE running buffer at typically 120 V for 20 minutes, depending on the fragment size. DNA fragments were finally visualized under UV light on a transilluminator and photographed using Molecular Imager, Gel DOC TM Imaging System, BioRAD.

4.3.4. Cleaning of PCR Product

PCR products that showed a clearly distinguished band on gel underwent cleaning using enzymatic PCR cleanup method or known as ExoSAP method. This method uses the two enzymes; Exonuclease I enzyme (New England Biolabs, Cat# M0293L), which acts to remove leftover primers, and Antarctic Phosphatase enzyme (New England Biolabs, Cat# M0289L), which removes any remaining dNTPs. For each PCR clean up reaction, a total volume of 7µl is needed, 0.25µl of Antarctic phosphatase and 0.025µl of Exonuclease I were mixed with 1.725µl of nuclease-free water. Sufficient master mix, containing all maintained reagents except PCR product, was prepared for the number of planned reactions. This was followed by aliquoting 2ul of the mix into each reaction well, followed by the addition of 5 ul of the PCR product.

ExoSAP method was carried out in the thermocycler using the following PCR cleaning program:

Step 1: 37 ºC for 30 min, **step 2:** 80 ºC for 20 min., and **Step 3:** 4 ºC for ∞.

4.3.5. Sequencing of the Cleaned PCR Product

The sequencing reaction was optimized using 0.5µl of the BigDye® Direct Cycle Sequencing Kit (Applied Biosystems, Cat# 4336768), 1.0µl of the 5X buffer (Applied Biosystems, Cat# 4336697) and 0.5 µl from each of the forward and the reverse primers, mixed with 5µl nuclease-free water and 1 ul of the cleaned PCR product. A reaction mixture sufficient for the number of reactions, excluding the templates, was prepared. This was followed by aliquoting 7µl of the mixture into each reaction well, followed by the addition of the purified PCR product.

The sequencing reactions were carried out in the thermocycler using the following sequencing PCR program:

Step1 (1 cycle):	Initial denaturation at 96 ºC for 3 min		
Step2 (30 cycles):	Denaturation	Annealing	Extension
	96 ºC for 10 sec	50 ºC for 5 sec	60 ºC for 2 min
Step 3 (Hold)	4 ºC for ∞		

4.3.6. Cleaning of the Sequenced PCR Product and Capillary Electrophoresis

Sequencing products were cleaned using EDTA/ethanol method by which 60µl of the 100% absolute ethanol and 5µl of 125 mM EDTA (Amresco-Cat # 0720) were added to each sequencing reaction, followed by incubation for 20 minutes at -20^{o}C. This step aims to precipitate the sequenced PCR reaction fragments. The samples were then centrifuged at 3800 rpm for 30 minutes at 4^{o}C. The supernatant was discarded and 100µl of 70% ethanol was added to each reaction and centrifuged again at the same conditions for 20 minutes. The samples were then inverted on clean tissue paper and were centrifuged at 500 rpm for 1 minute to get rid of any

residual supernatant. The samples were dried at 95°C for 5 minutes to evaporate residual ethanol, followed by the addition of 12µl HiDi Formamide (Applied Biosystems, Cat# 4311320). The samples were vortexed and heated again at 95°C for 5 minutes. Finally, the samples were immediately transferred into ice block for another 5 minutes and were later loaded onto the sequencing plate. At last, samples were run on ABI 3130 Genetic Analyzer (Applied Biosystems, S/N:20355-023) capillary electrophoresis.

4.3.7. Analysis of Sequencing Data

At the end of the capillary electrophoresis running time, sequencing data were obtained, and for each sequencing reaction, a file was generated and recorded on the computer. These files were viewed using DNA Chromatogram Software, and the resulting sequences were aligned against the web-based human reference genome (UCSC, Human GRCh37/hg19). Bioinformatic tools such as PolyPhen-2 v2.2.2 (http://genetics.bwh.harvard.edu/pph2/) and SIFT (http://sift.jcvi.org/) were utilized in order to predict the impact of missense SNPs on the structure and function of proteins. Another frequently used tool was ExAC (http://exac.broadinstitute.org), used as a reference set of allele frequencies for disorder analyses.

4.4. Haplotype Analysis using Microsatellite Markers

4.4.1. Identification of STR Loci and Primer Design

To obtain Short Tandem Repeat markers sequences around *SNX10* gene loci, hg19 assembly in UCSC Genome Browser was used to display all microsatellite markers in a chromosomal coordinate window of 2Mb (2,000,000 bases) downstream and upstream of the gene sequence. Potential STR markers were selected based on the following criteria:

(i) Selected STR markers were long enough and have suitable flanking regions to place PCR primers in.

(ii) To increase the chance of choosing highly polymorphic markers highly motif nucleotide repeat number STR were selected.

(iii) Some repeat motifs that are hard to amplify and tend to form strong secondary structures (e.g., GC/CG, TAA/ATT) were avoided.

After applying the mentioned filtering criteria, six short tandem repeat (STR) markers around the SNX10_p.R51Q locus (as shown in Table 3) were selected, by which the first three STR are located before the SNX10_p.R51Q gene locus, and the other three STR are in front of this gene locus. Primer pairs were designed for all the selected markers' sequences using Hemi-NeSTR website with default parameters.

Table 3. *SNX10* gene STR Markers: The table illustrates markers codes and their positions arranged related to *SNX10* gene position.

Chr	position hg19	Repeat	Marker Code	Distance from mutation	Amplicon size
chr7	**25021737**	**22xTG**	**M10**	**-1309778**	**173bp**
chr7	**25670483**	**20xTG**	**M20**	**-661032**	**114bp**
chr7	**25896549**	**20xAC**	**M25**	**-434966**	**164bp**
***SNX10* gene**					
chr7	**27292064**	**24xGT**	**M45**	**960549**	**215bp**
chr7	**27373235**	**22xGT**	**M48**	**1041720**	**116bp**
chr7	**27746057**	**24xAC**	**M54**	**1414542**	**138bp**

Each STR marker were amplified in separate reactions by polymerase chain reaction (PCR) in 25µl reaction volumes containing the followings:

Table 4. Haplotype PCR Recipe

Reagents	**Quantity per 1X (µl)**
Forward primer with 5' FAM tail *	0.1
Reverse primer	0.5
Universal FAM dye	0.5
Polymerase Buffer	2.5
dNTPs	2.0
DMSO (Q solution)	2.0
Taq polymerase	0.25
MgCl2 Buffer	1.0
N.F water	15.15
DNA template	1.0

*FAM universal sequence is: GTCGGTGCAGAGCATCATGC

Selected markers were tested on families carrier for the SNX10_p.R51Q variant, by which, one homozygous patient for SNX10_p.R51Q, one heterozygous sibling, and both parents were picked to undergo homozygosity mapping. Thus, the PCR master mix (without DNA template) was prepared for each marker alone to be sufficient for all the family members plus one NTC reaction. The amplification profile was composed as follows: 2 min at 94˚C, 35 cycles of 30 seconds at 94˚C, 60 seconds at 55˚C, 60 seconds at 72˚C, followed by a final extension step of 10 minutes at 72˚C.

4.4.2. Haplotype Genotyping and Fragment Analysis Procedure

After PCR reaction, PCR reaction dilution was followed to reduce the intensity and get better and clear peak on the Genetic Analyzer machine, the dilution was done by 1:10 ratio by taking

1µl of PCR product and add to it 9µl of nuclease-free water. After that, the diluted PCR product was mixed with 0.25µl GeneScan™ 500 ROX™ Dye (an internal lane size designed for sizing DNA fragments during capillary electrophoresis), and 10.75µl of HiDi (highly deionized Formamide used to resuspend samples before electrokinetic injection in capillary electrophoresis systems). The mixture (diluted PCR product, ROX dye, and HiDi) was heated for 5 minutes on 95 ^{o}C for denaturation. Immediately, the mixture was placed on ice block to stop denaturation and prevent the DNA strands from annealing again. Finally, the reaction mixture was run for around one hour on the capillary electrophoresis (CE) system, and then analyzed using GeneScan Software on the 3130XL Genetic Analyzer. At the end, haplotype analysis was done for each family to detect length variation in the chosen STR markers.

4.5. Whole-Exome Sequencing

Whole exome sequencing was performed at Hereditary Research Laboratory using Illumina's NextSeq™ 500 Sequencing System. DNA library was prepared using the Illumina® TruSeq™ DNA Sample Prep Kit, which provides coverage of 45 Mb of exonic content.

First of all, the initial genomic DNA samples were quantified using Qubit® Fluorometer (Life Technologies, Cat# Q32866), and quality checked by gel electrophoresis. gDNA were then normalized to 100 ng needed for the shearing process using the Covaris M220 Focused-ultrasonicator™ (Covaris, Cat# 500295). After the shearing process, dsDNA fragments with 3’ or 5’ overhangs were generated. The resultant overhangs were converted into blunt ends using End Repair Mix (Illumina, Part# 15012494), which acts to remove the 3’ overhangs while the polymerase activity fills in the 5’ overhangs. A single 'A' nucleotide was added to the 3' ends of the blunt fragments using A-Tailing Mix (Illumina, Part# 15012495) to prevent them from

ligating to each other during the adapter ligation reaction. This was followed by ligating multiple indexing adapters that have a corresponding "T" nucleotide on their 3' end, which provides a complementary overhang for ligating the adapter to the fragment. And the ligated indexing adapters prepare the DNA fragments for hybridization onto a flow cell. The DNA fragments were then amplified by PCR using primers (PCR Primer Cocktail, Illumina, Part# 15021793) that selectively enrich the DNA fragments with ligated adapters on both ends. A library size of an average 300 bp was then selected using Sample Purification Beads (Illumina, Part# 15037172). The library quality of each sample was checked using Agilent 4200 TapeStation System (Agilant, Cat# G2991AA) which gives the average size and concentration measurements. DNA libraries harboring unique indexes were combined into a single pool, followed by hybridization of the targeted exonic regions using capture probes (Coding Exome Oligos, Illumina, Part# 15034575). Subsequently, the hybridized probes were then captured using Streptavidin Magnetic Beads (Illumina, Part# 15015927). Two wash stages were done to eliminate non-specific products. Hybridization, capture and wash steps were then repeated to guarantee specificity. A final round of PCR amplification was performed to amplify the enriched library. After the final quality and quantity control using Agilent 4200 TapeStation System, the normalized, pooled library was loaded onto NextSeq500 for a target of ~100 million 2x76 paired-end reads per sample.

After library sequencing on Illumina NextSeq500 platform, the produced 256,398,494 reads (FASTQ files format) were aligned to Genome Reference Consortium Human Build 37 (GRCh37/hg19) using Burrows-Wheeler Aligner (BWA) (bio-bwa.sourceforge.net). Mapped reads (BAM format) went through preprocessing steps by removing PCR duplicates, realigning

around indels, and recalibrating base quality. SNPs, indels, CNVs calls were generated using ANOVAR tool. Prioritization of variants to identify the causative mutation was done after filtering out variants with read depth less than 10 (low coverage), and minor allele frequency of more than 0.1% on ExAC (http://exac.broadinstitute.org). Rare variants were filtered against their presence in known databases such as 1000 Genome Project (http://www.1000genomes.org). To sort potentially deleterious alleles from benign polymorphisms, effects of the variants were predicted on the protein level by Polyphen2, and SIFT tools. Potentially deleterious allele/alleles (that have a damaging effect on the protein level) were tested for segregation in the families.

CHAPTER 5

Results: Clinical and Genetic Analysis of Families

5.1. Clinical Assessment and Pedigree of Family 1

Family 1 (OST-A) individuals were recruited from Yatta region (south of Hebron) and comprehensive interviews were conducted with family members for pedigree construction, as indicated (Figure 5). Three affected female children from this consanguineous family were referred to us initially for genetic diagnosis with clinical manifestations of ARO. Patients A/IV-2 and A/IV-1 (Figure 5) were both deceased. Patient A/IV-1 was admitted to Yatta Hospital post-delivery as a case of poor feeding and she was kept on NGT feeding for one week. She was found to have poor weight gain, increased bone density by X-ray, and dysmorphic features. Later she developed a life-threating anemia, thrombocytopenia, leukocytosis, splenomegaly, and bilateral congenital cataracts. She was referred to Al-Makassed Hospital for evaluation and she was diagnosed with severe infantile form of osteopetrosis. At approximately 9 months old, she suffered from acute E. coli infection with high fever, and died as a result of septic shock. Her sibling, patient A/IV-2 was referred to Alia Hospital after birth, she had poor vision, and poor weight gain. She had wide depressed atrial fibrillation, hairy forehead, long eyelashes, anteverted nostrils, long philtrum, Broad alveolar ridges, and very stiff joints. She was diagnosed with osteopetrosis because of her similarly affected sister.

After two years of investigation and intensive work of disease gene identification, we were informed that A/IV-2 patient was died at age of almost 2 years old, and that the family had given birth to another affected female, A/IV-3. A/IV-3 is now 6 months old, and she is alive as of the

time of this report, and she is still in follow-up. She was also diagnosed as osteopetrosis patient because of the similar phenotypic features of her siblings.

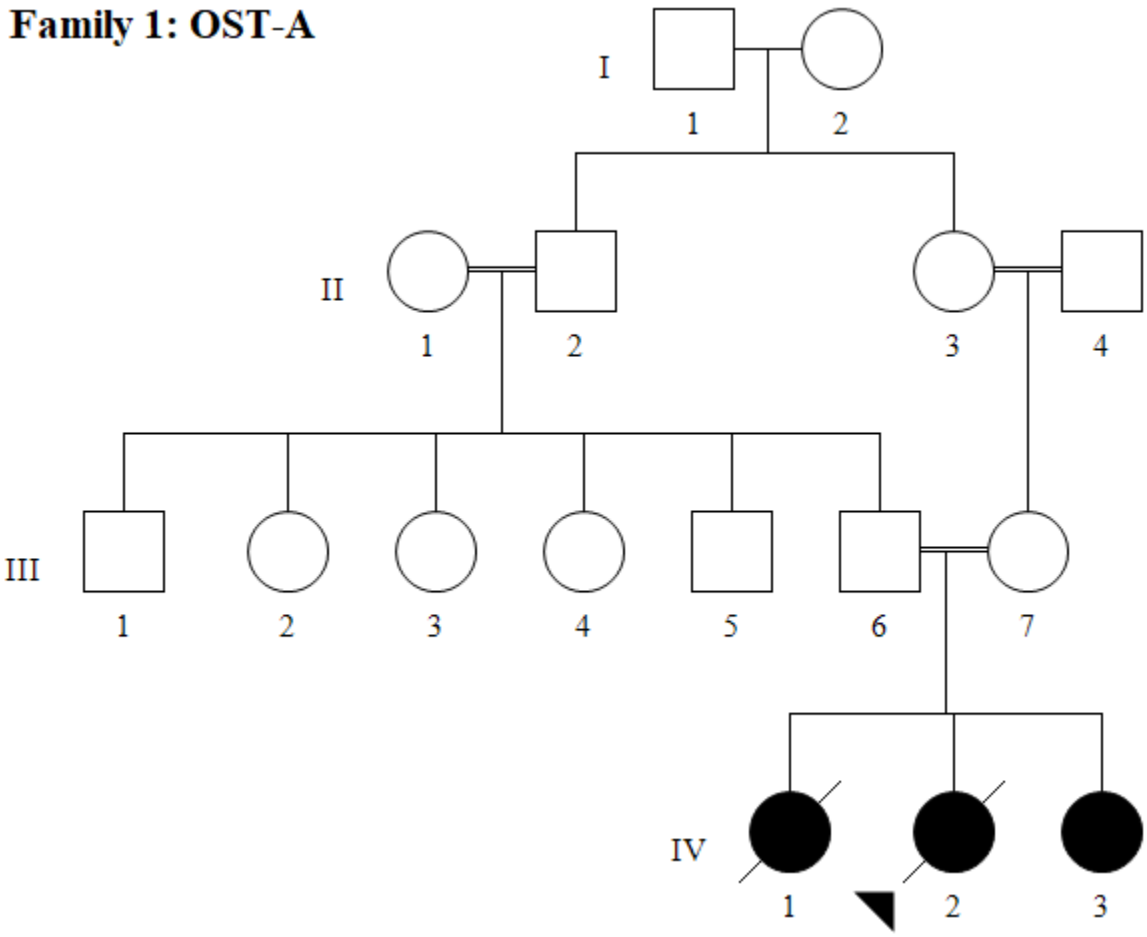

Figure 5: Pedigree of family 1 (OST-A) with Malignant Infantile Osteopetrosis, showing affection status of sampled individuals.

5.1.1. Whole-Exome Sequencing Analysis Results in Family 1

Individual A/IV-2 underwent whole-exome sequencing. Rare variants were filtered against their presence in known databases such as The Exome Aggregation Consortium (ExAC) ,1000 Genomes Project, Exome Variant Server. Analysis focused on prioritizing nonsense, splice-site, Indels in coding regions, and nonsynonymous variants.

To sort potentially deleterious alleles from benign polymorphisms, effects of the variants were predicted on the protein level by Polyphen2, SIFT and REVEL tools. Potentially deleterious allele/alleles were tested for segregation in Family 1. Segregation was performed for all the variants that met the filtering criteria and fit the phenotype as shown in Table 5. but unfortunately, none of the variants segregate with the phenotype in the family members.

Table 5. Candidate variants and their segregation in the family with the phenotype

Gene	Function	Mutation	Segregation
1- SNX10	Exonic, nonsynonymous	p.R51Q	Did not Segregate
2- CLCN7	Exonic, nonsynonymous	p.G521R	Did not Segregate
3- ADCY6	Exonic, nonsynonymous	p.I1106M	Did not Segregate
4- GNAS	Exonic, nonsynonymous	p.E357Q	Did not Segregate
5- KRT82	Exonic, Stopgain	p.Y315X	Did not Segregate
6- PMEL	Exonic, nonsynonymous	p.R192Q	Did not Segregate
7- ERCC2	UTR5	c.-325T>C	Did not Segregate

5.2. Clinical Examination of Families 2, 3, 4, 5, 6, 7, 8, 9

Eight families displaying osteopetrosis were seen from Al-Karma, Hebron city. All of the eight families share the same clan, and same family name. Upon interviewing, they did not deny the possibility of sharing a common ancestor but could not however, trace the relatedness despite the frequent consanguineous marriages within each family. Diagnosis was based mainly on clinical examination and panoramic X-rays when present. Similar findings in all eight families suggested a common etiology. Early disease manifestation is a common finding in severely affected

osteopetrosis individuals. They are born to unaffected parents, and the phenotype tends to be inherited in an autosomal recessive manner.

The affected individuals displayed systemic findings suggesting that they display the most severe form of osteopetrosis which is the malignant infantile form of osteopetrosis (ARO). The most prominent features of those individuals were:

- Facial characteristics and dysmorphic features.
- Increased bone density “bone within bone appearance”.
- Multiple fractures of legs and ribs.
- Vision problems, some have unilateral or bilateral visual loss.
- Enlarged spleen and liver.
- Routine blood tests usually show elevated leucocytes and decreased red cells, platelets and hemoglobin.
- Acute infections.

The respective pedigrees of Al-Karma families are shown in figures 6, 7, 8, 9, 10, 11, 12 and 13. A summary of clinical findings in the affected individuals, showing also who underwent bone marrow transplantation, can be found in Table 6.

Table 6. Clinical findings of AL-Karma patients

Family #	Family Code	Patient	Gender	Current Age (Years)	Hearing	Eyesight	BMT
2	**OST-B**	B/III-13	Male	7 years	Intact	Intact	Failed BMT at 2 years
3	**OST-C**	C/IV-4	Female	10 years	Intact	Bilateral visual loss	Not Done
4	**OST-D**	D/III-3	Male	6 years	Intact	-	Not Done
5	**OST-E**	E/II-1	Male	Died at 11 years	Intact	-	-
6	**OST-F**	F/III-5	Male	9 years	Intact	Partial visual loss	Not Done
7	**OST-G**	G/III-9	Male	16 years	Intact	Unilateral visual Loss	Successful BMT
8	**OST-H**	H/II-3	Female	6 years	Intact	-	-
9	**OST-I**	I/II-2	Male	3 years	Intact	Bilateral visual loss	Failed BMT at 8 months

BMT, bone marrow transplantation

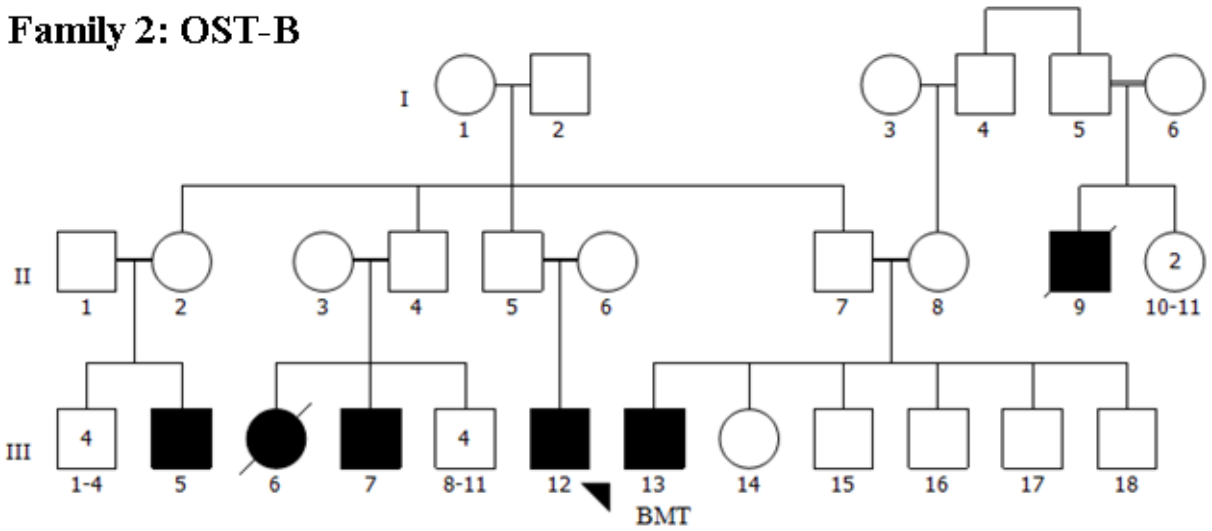

Figure 6: Pedigree of family 2 (OST-B) with Malignant Infantile Osteopetrosis, showing affection status of sampled individuals.

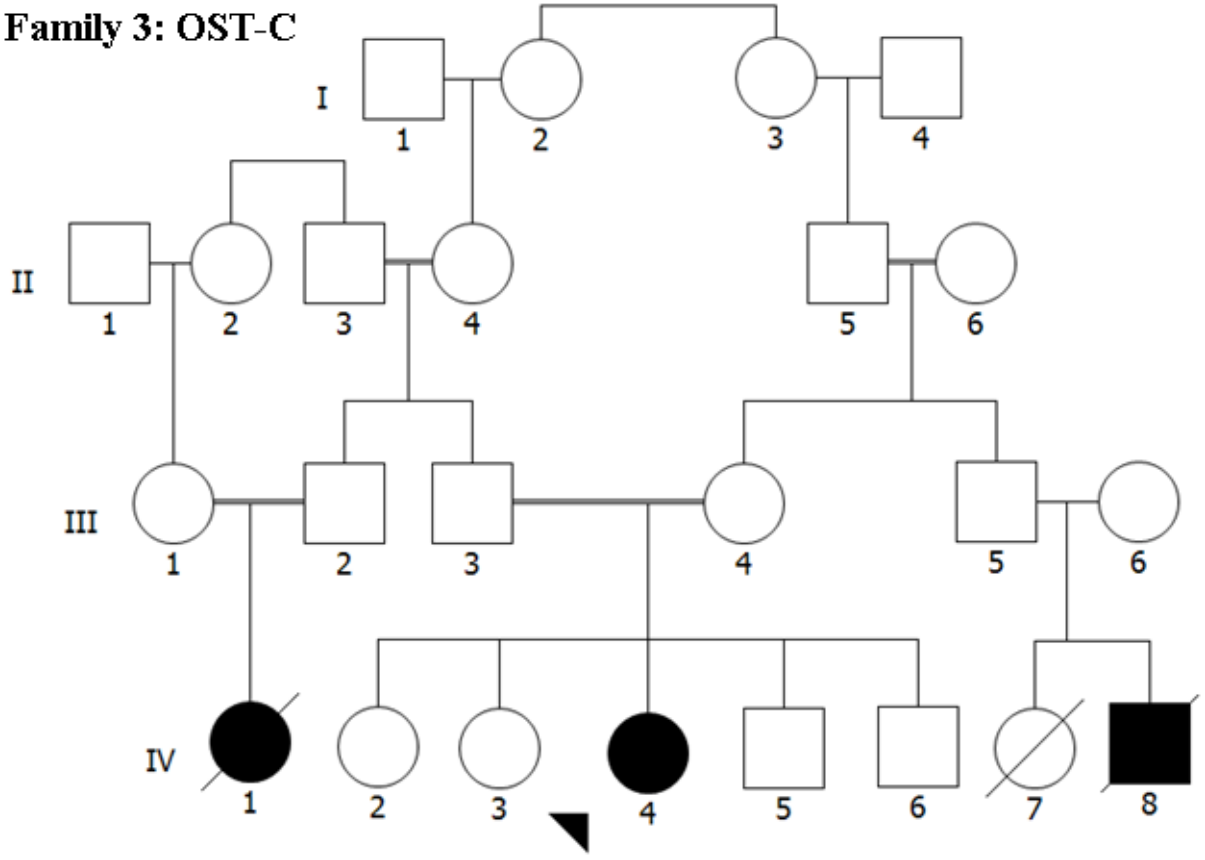

Figure 7: Pedigree of family 3 (OST-C) with Malignant Infantile Osteopetrosis, showing affection status of sampled individuals.

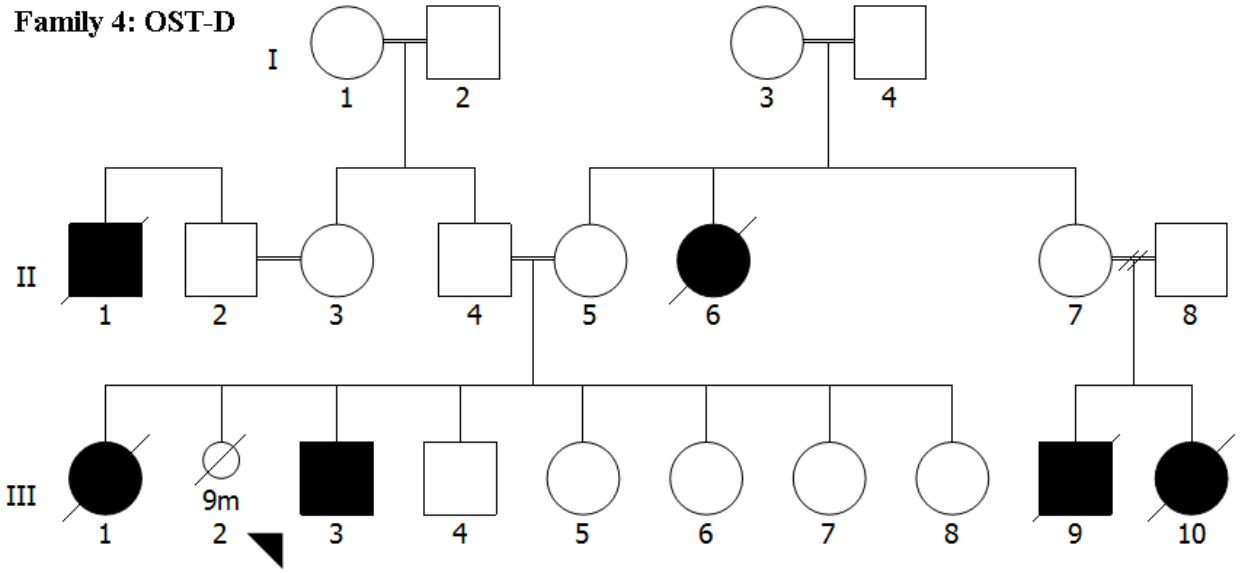

Figure 8: Pedigree of family 4 (OST-D) with Malignant Infantile Osteopetrosis, showing affection status of sampled individuals.

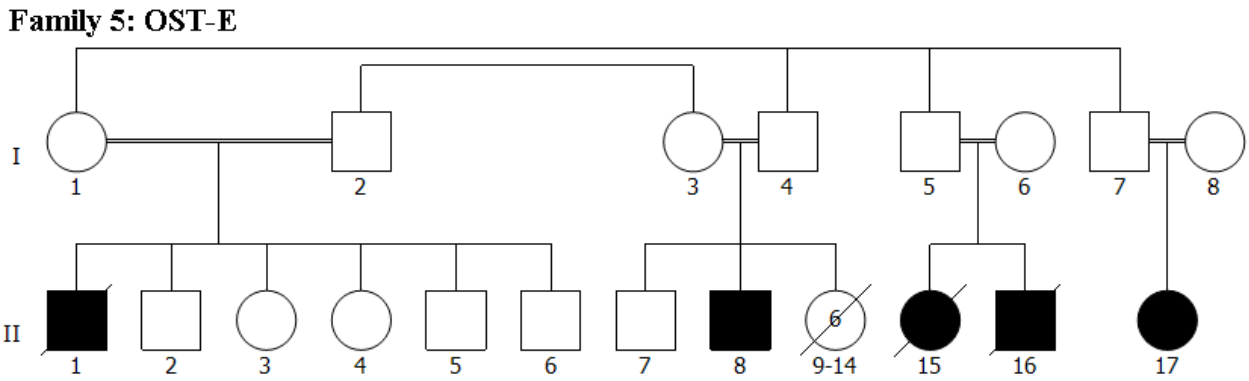

Figure 9: Pedigree of family 5 (OST-E) with Malignant Infantile Osteopetrosis, showing affection status of sampled individuals.

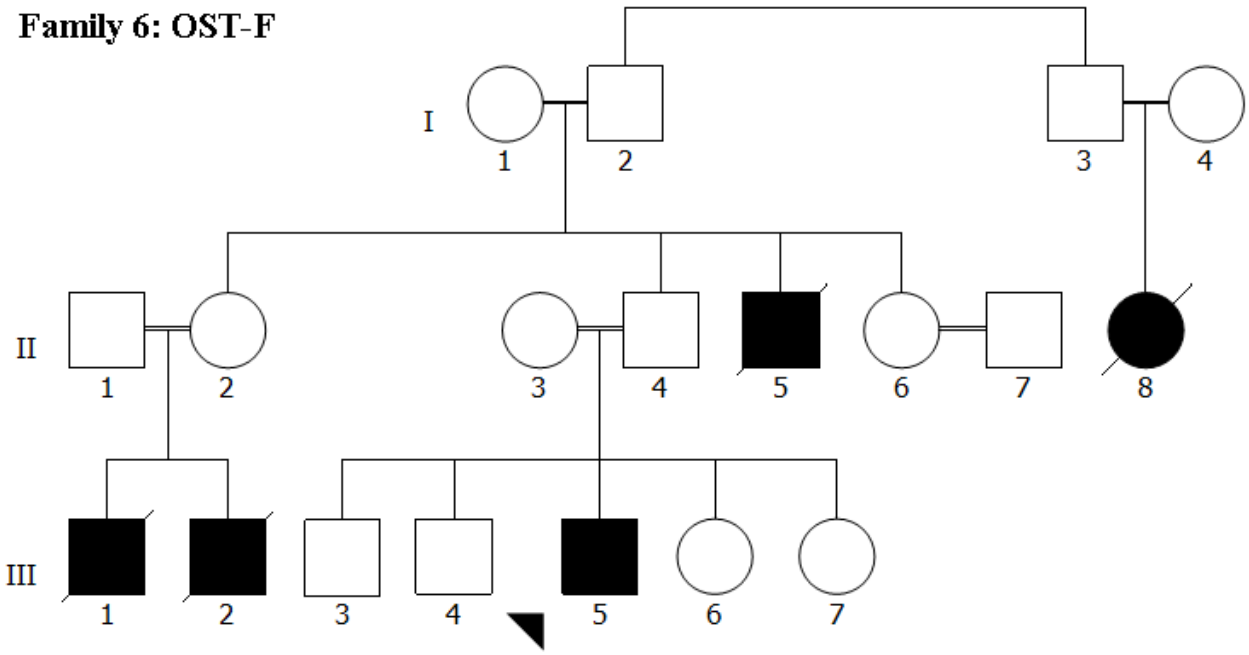

Figure 10: Pedigree of family 6 (OST-F) with Malignant Infantile Osteopetrosis, showing affection status of sampled individuals.

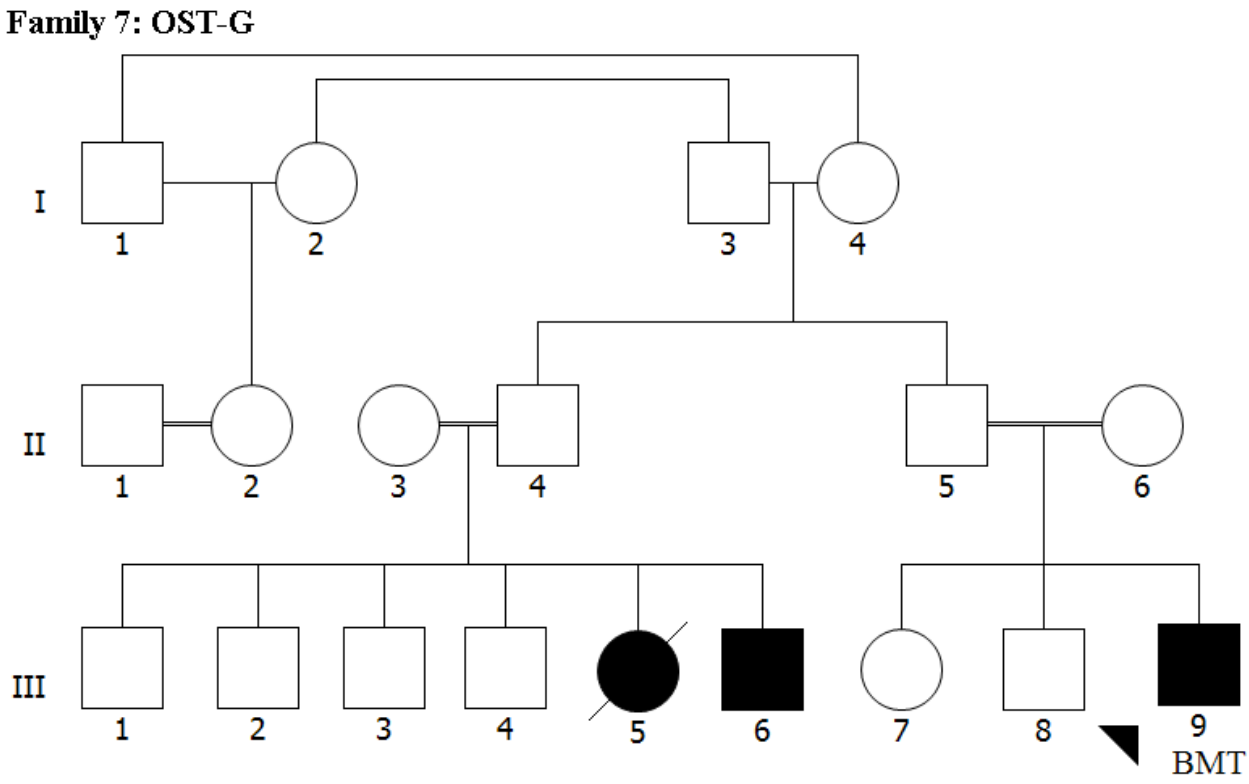

Figure 11: Pedigree of family 7 (OST-G) with Malignant Infantile Osteopetrosis, showing affection status of sampled individuals.

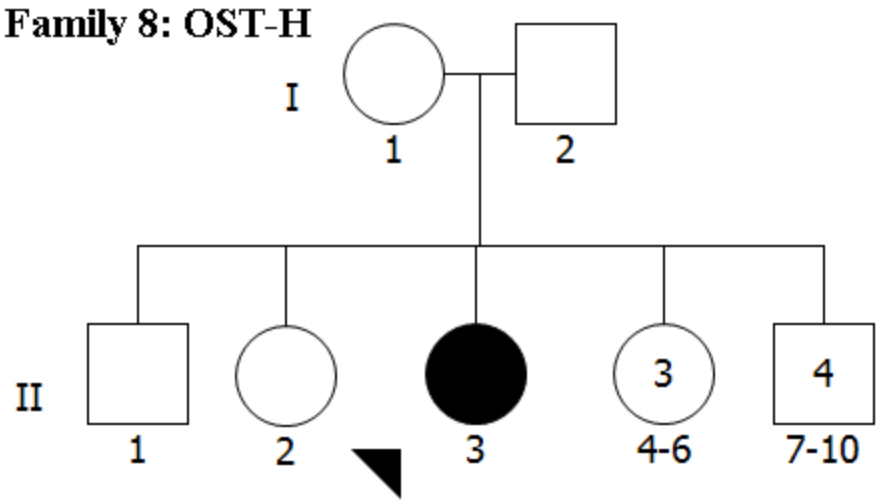

Figure 12: Pedigree of family 8 (OST-H) with Malignant Infantile Osteopetrosis, showing affection status of sampled individuals.

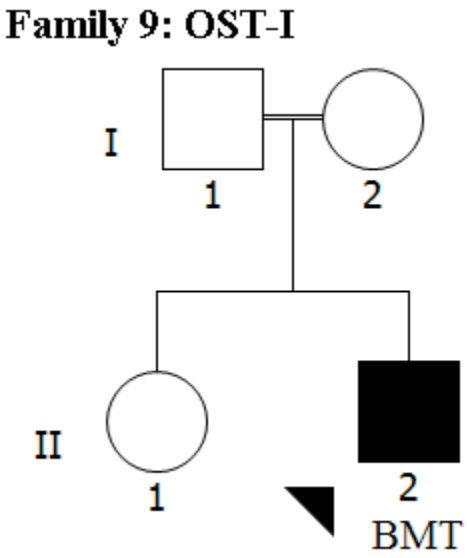

Figure 13: Pedigree of family 9 (OST-I) with Malignant Infantile Osteopetrosis, showing affection status of sampled individuals.

5.2.1. Exome Sequencing Analysis Results in Family7

Exome Sequencing of two osteopetrosis affected cousins of G/III-9 was performed at the Center for Clinical Genetics department at Hadassah Medical Center, using a HiSeq2500 Illumina platform. Exome sequencing was performed on genomic DNA samples belonging to the two affected cousins. After filtering out of variants with low coverage, synonymous, predicted benign by MutationTaster. And those with minor allele frequency of more than 0.1% in the ExAC database, a homozygous variant was identified in both affected cousins, namely c.152G> A (p.Arg51Gln) in the *SNX10* gene, and it co-segregated with the phenotype in the family. The mutation p.Arg51Gln is found in a highly conserved residue in the gene *SNX10*. Mutations in *SNX10* gene are known to cause Malignant Infantile Osteopetrosis ARO (Aker et al., 2012).

5.2.2. Sanger Sequencing Results of Candidate Variant p.R51Q (c.152G> A) in *SNX10* gene in Family2, 3, 4, 5, 6, 7, 8, 9

To assess the causality of the homozygous c.152G>A (p.R51Q) variant in the *SNX10* gene that was identified by WES in the affected cousins of G/III-9 in Family7, the target DNA base positions (SNX10 mRNA accession number NM_001199835.1) and their flanking sequences were amplified from DNA samples of family members using the primers in Table 7 (refer to Appendix I for primer sequences). The PCR products were later sequenced in both forward and reverse directions as shown in Figure 14.

Segregation analysis confirmed that the *SNX10* p.R51Q variant was present in almost all affected individuals (B/III-13, C/IV-4, D/III-3, E/II-1, F/III-5, G/III-9, and I/II-2) who have been diagnosed with osteopetrosis, and their unaffected parents were heterozygous carriers. The only exception is the affected individual H/II-3 in Family8, who was Wildtype for *SNX10*_p.R51Q

variant. Segregation results are shown in the detailed pedigrees of Al-Karma families in Figures 15, 16, 17, 18, 19, 20, 21 and 22. It should be noted that ARO patients who did Bone Marrow Transplantation (BMT), takes a donor's healthy blood-forming cells and puts them into the patient's bloodstream, where they begin to grow and make healthy red blood cells, white blood cells and platelets. As White Blood Cells were used for DNA extraction, a BMT patient could have a pure WBC population of the donor's genotype, or he could have some residual bone marrow which gives rise to his own WBC genotype and therefore he would have mixed WBC populations. This means that, we have 3 scenarios outcome for BMT ARO patient's genotype of *SNX10*_p.R51Q variant; either normal wildtype for *SNX10*_p.R51Q, heterozygous for *SNX10*_p.R51Q, or homozygous for *SNX10*_p.R51Q.

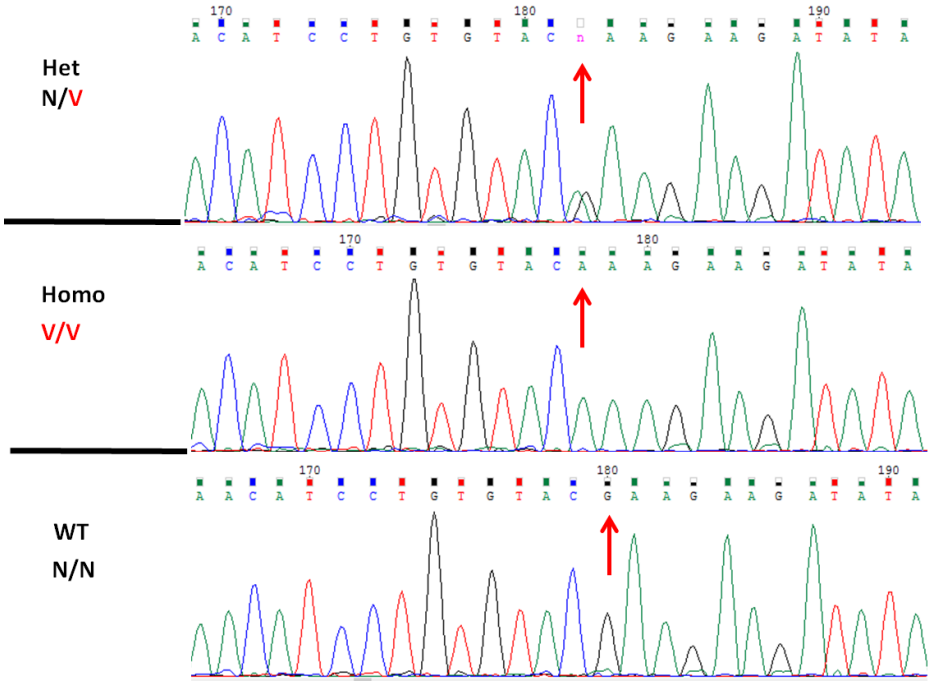

Figure 14: Sanger sequencing results of exon 4 of *SNX10* gene showing the wildype and heterozygous and homozygous chromatogram for p.R51Q variant.

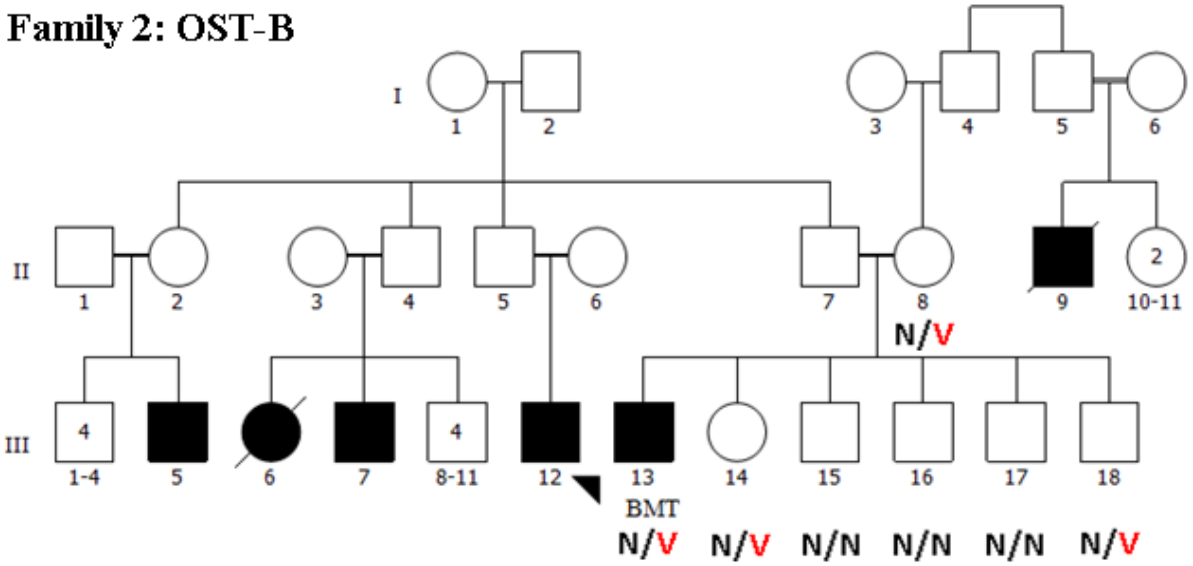

Figure 15: Pedigree of family 2 displaying SNX10_p.R51Q genotype of sampled individuals. Highly consanguineous marital relationships produce offspring with two copies of the mutant SNX10 allele that segregate with ARO phenotype. B/III-13 ARO patient did bone marrow transplantation, and thus the wildtype allele that he has belongs to the healthy donor who donated the bone marrow.

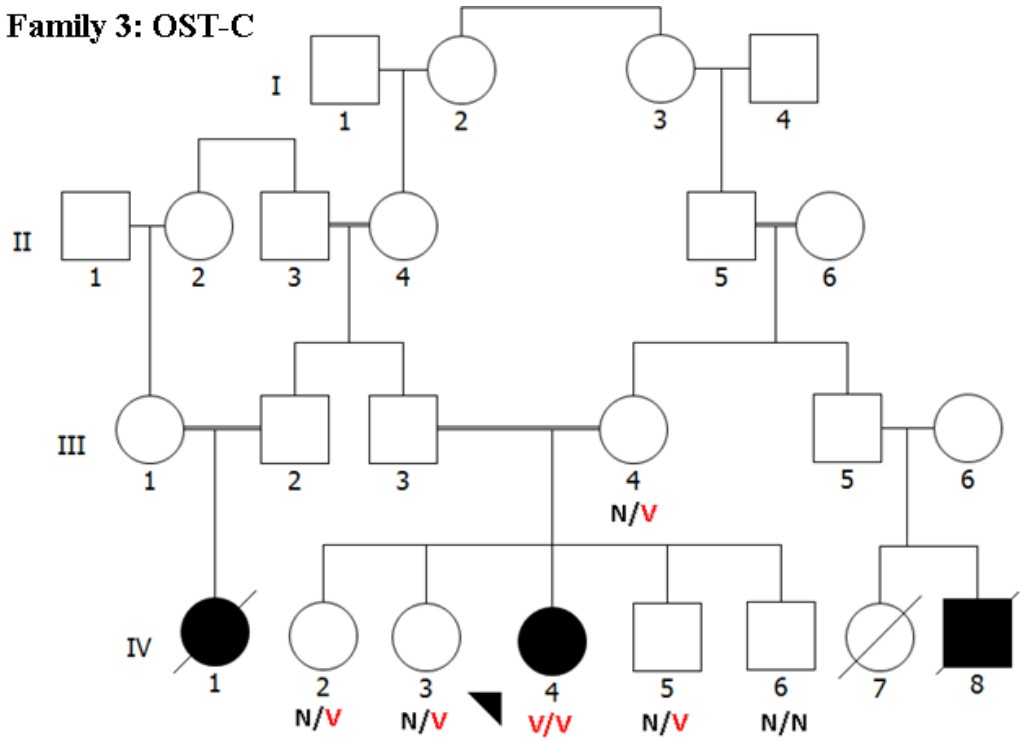

Figure 16: Pedigree of family 3 displaying SNX10_p.R51Q genotype of sampled individuals. Highly consanguineous marital relationships produce offspring with two copies of the mutant SNX10 allele that segregate with ARO phenotype in C/IV-4 individual.

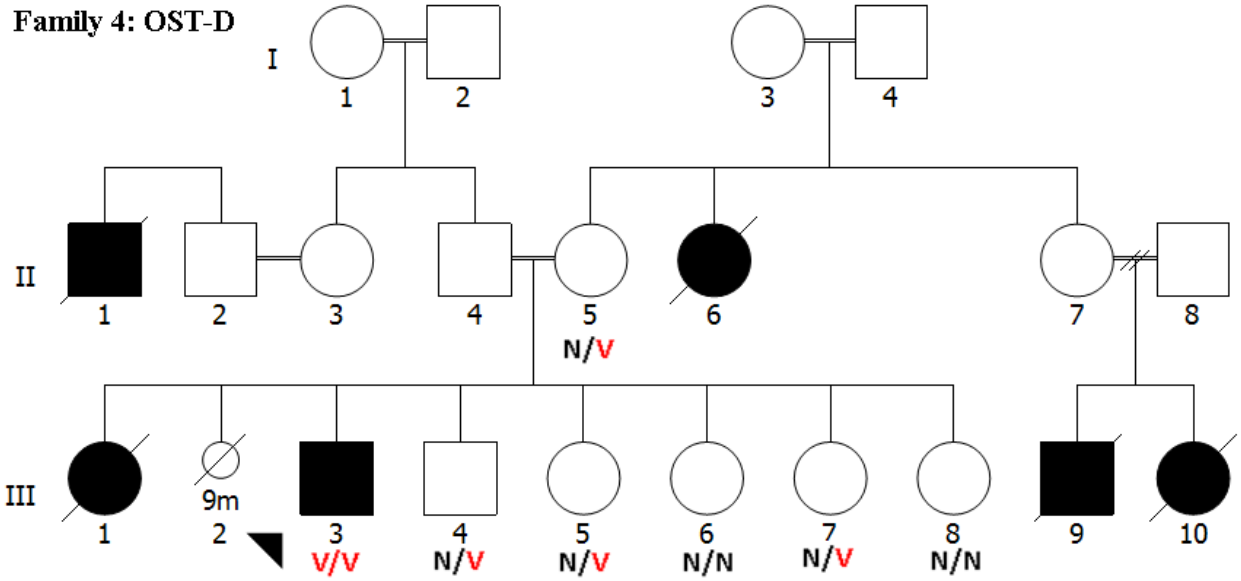

Figure 17: Pedigree of family 4 displaying *SNX10* genotype of sampled individuals. Affected individual (D/III-3) is homozygous for SNX10_p.R51Q mutation.

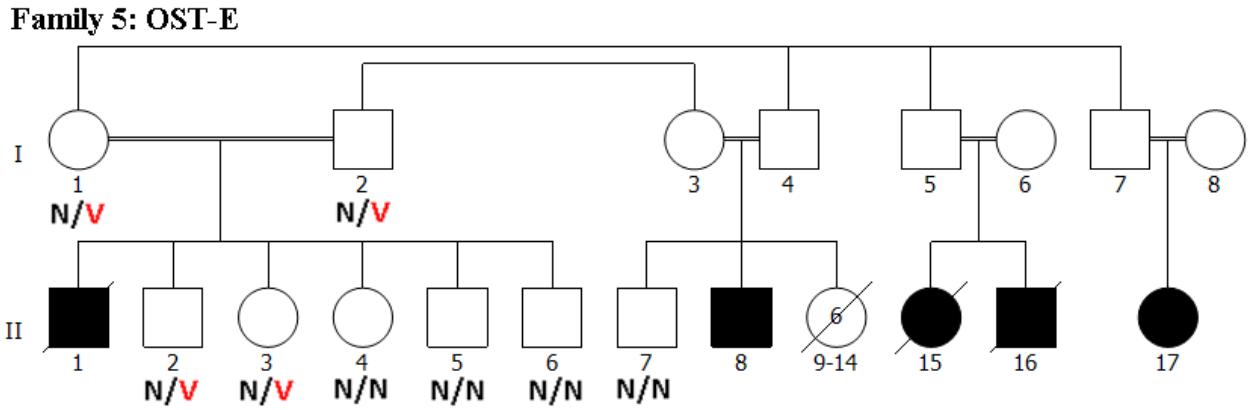

Figure 18: Pedigree of family 5 displaying *SNX10*_p.R51Q genotype of sampled individuals. Heterozygous SNX10_p.R51Q variant carriers display no osteopetrosis phenotype, but can give rise to osteopetrosis offspring in an autosomal recessive inheritance manner.

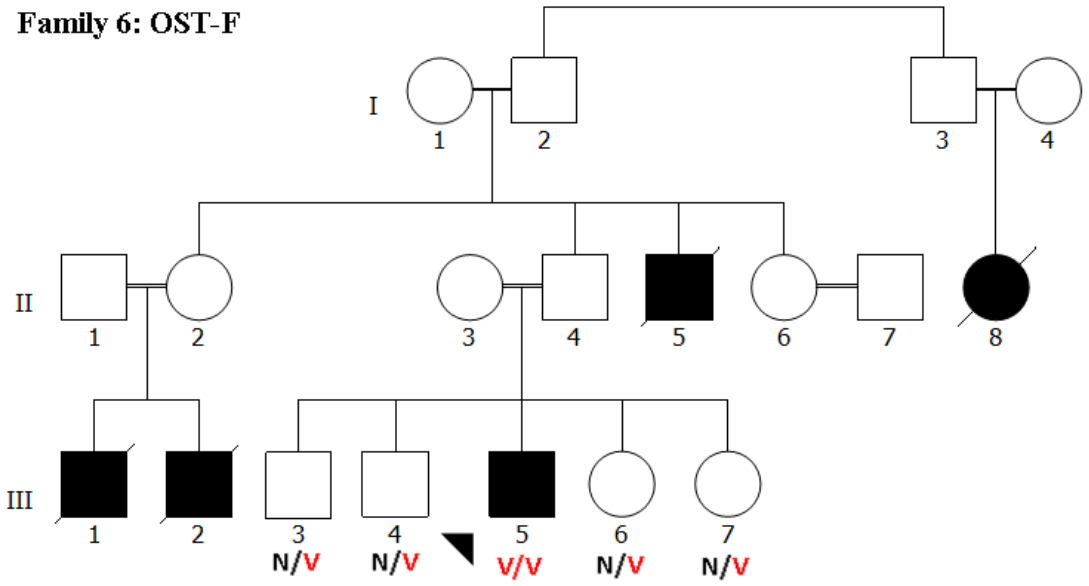

Figure 19: Pedigree of family 6 displaying *SNX10* genotype of sampled individuals. Affected individual (F/III-5) is homozygous for SNX10_p.R51Q mutation.

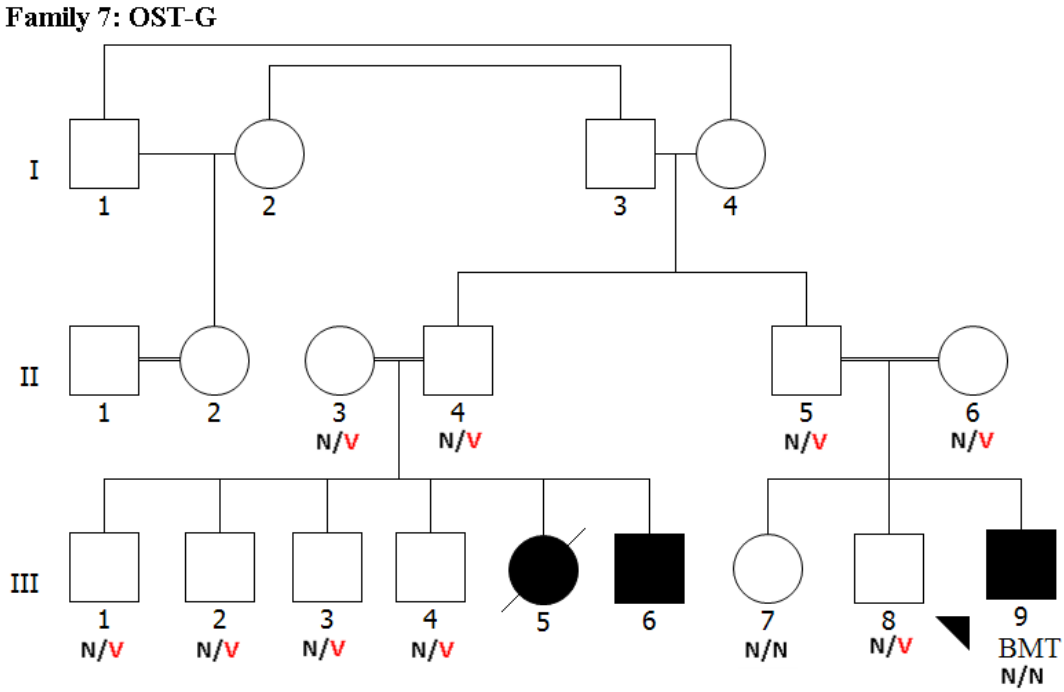

Figure 20: Pedigree of family 7 displaying SNX10_p.R51Q genotype of sampled individuals. Highly consanguineous marital relationships produce offspring with two copies of the mutant SNX10 allele that segregate with ARO phenotype. G/III-9 ARO patient did bone marrow transplantation, and thus the wildtype alleles that he has belong to the healthy donor who donated the bone marrow.

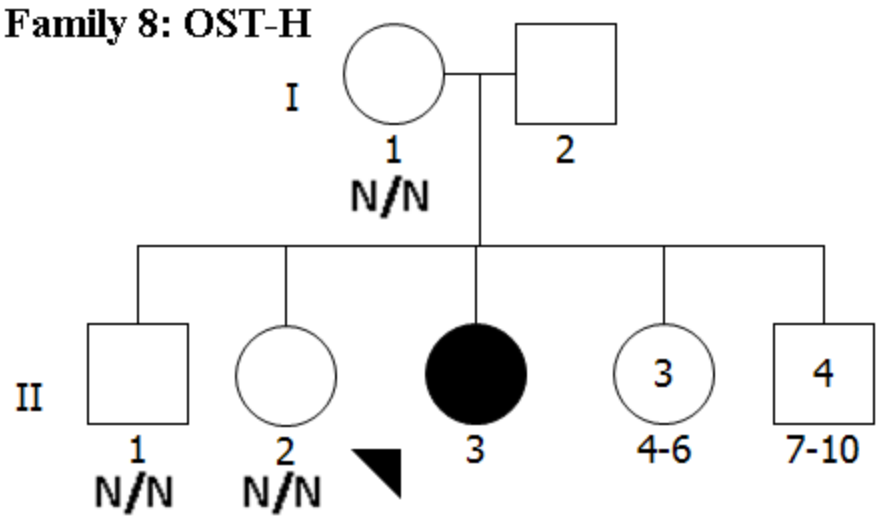

Figure 21: Family 8 (OST-H) belongs to the same clan of other Al-Karma families, yet all tested family members have the Wildtype allele for SNX10_p.R51Q variant.

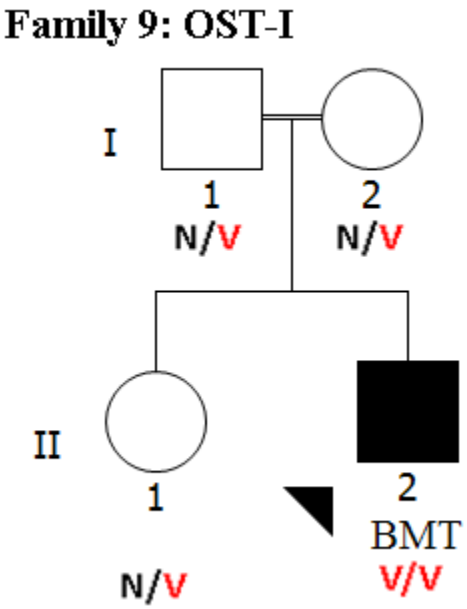

Figure 22: Pedigree of family 9 displaying *SNX10*_p.R51Q genotype of sampled individuals. Highly consanguineous marital relationships produce offspring with two copies of the mutant *SNX10* allele that segregate with ARO phenotype in I/II-2 individual.

5.2.3. Sanger Sequencing of the Coding Exons Sequences of *SNX10* Gene in Family8

DNA template of the affected individual H/II-3 was PCR amplified for the coding sequences of *SNX10* gene using the primers listed in Appendix I (Table 7). Sanger sequencing of the PCR product revealed a wild-type genotype.

5.2.4. Haplotype Analysis using Microsatellite Markers in Families 2, 3, 4, 5, 6, 7, 9, 10

Microsatellites or STR represent major type of haplotypes or molecular markers that can be used in genetic studies to trace the origin and evolution of the different mutations. Therefore, to trace the relatedness among Al-Karma families, and the possibility of sharing a common ancestor, haplotype analysis was done on these families. From each family, one affected patient homozygous for *SNX10*_p.R51Q, one heterozygous sibling for this patient, and his/her parents were picked to undergo homozygosity mapping. Family 10 (OST-J) were also screened for the same microsatellite markers as a control family, because it is from Ramallah and have different gene mutation as discussed later in this thesis. Six short tandem repeat (STR) markers around the *SNX10*_p.R51Q locus were screened, by which the first three STR are located before the *SNX10*_p.R51Q gene locus, and the other three STR are in front of this gene locus. STR markers were amplified by polymerase chain reaction (PCR) using fluorescent labeled primer and then examined by capillary electrophoresis (CE), and then analyzed using GeneScan Software on the 3130XL Genetic Analyzer. Finally, haplotype analysis were done for each family.

Haplotype analysis revealed that all Al-Karma patients who are homozygous for p.R51Q mutation were also homozygous for all studied markers around the *SNX10* gene locus, as indicated in Figure 23, and 24.

The minimum shared haplotype block linked to the mutation were determined (as shown in Figure 24), and this block was found in all the affected *SNX10* patients. And this means that the mutation originates in all the families from the same ancestry. Interestingly, different haplotypes were found in Family 10 (OST-J) as expected.

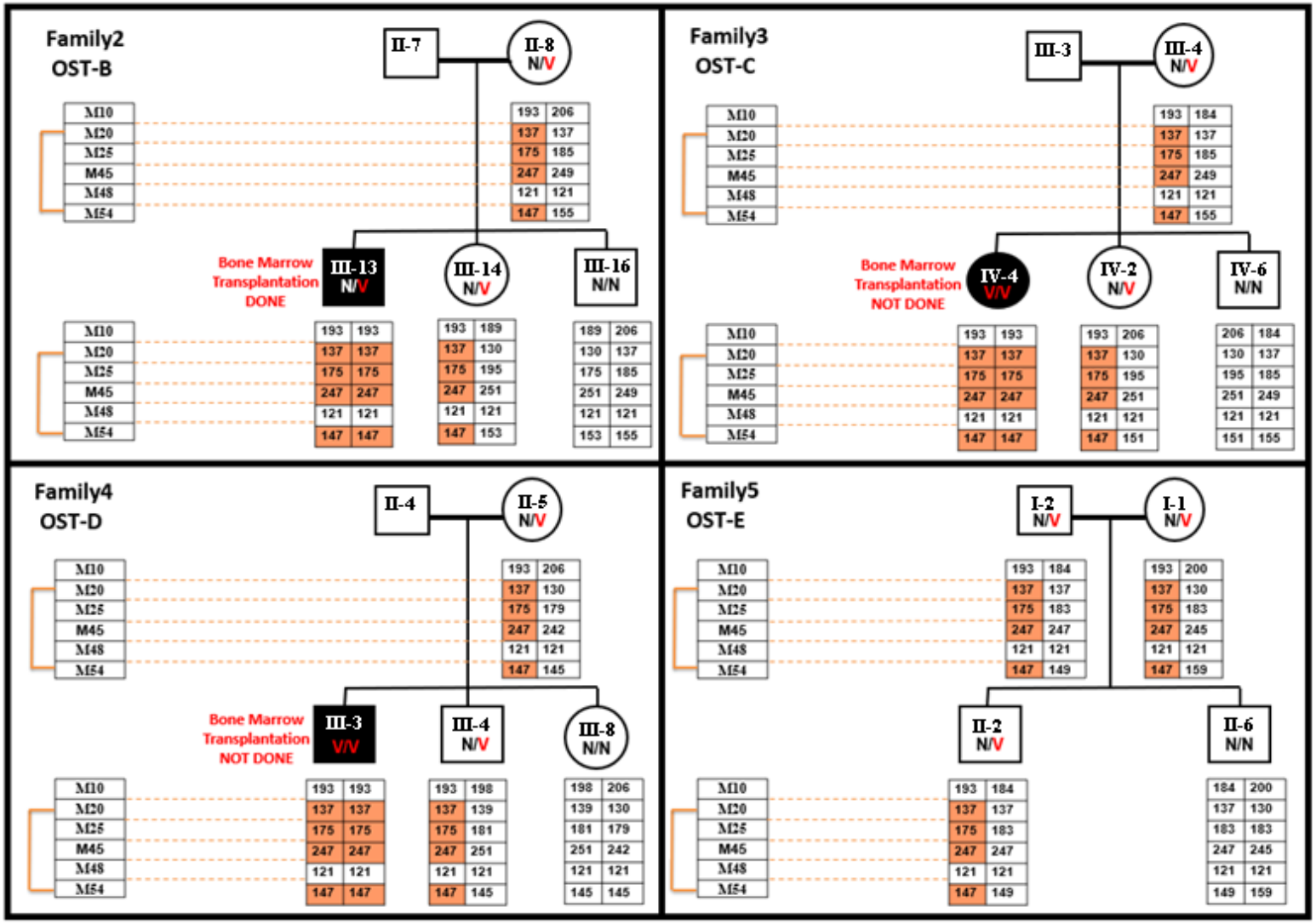

Figure 23: Haplotype analysis results for Families 2, 3, 4, and 5. Different colors mean different haplotypes while the same color indicates the same haplotype.

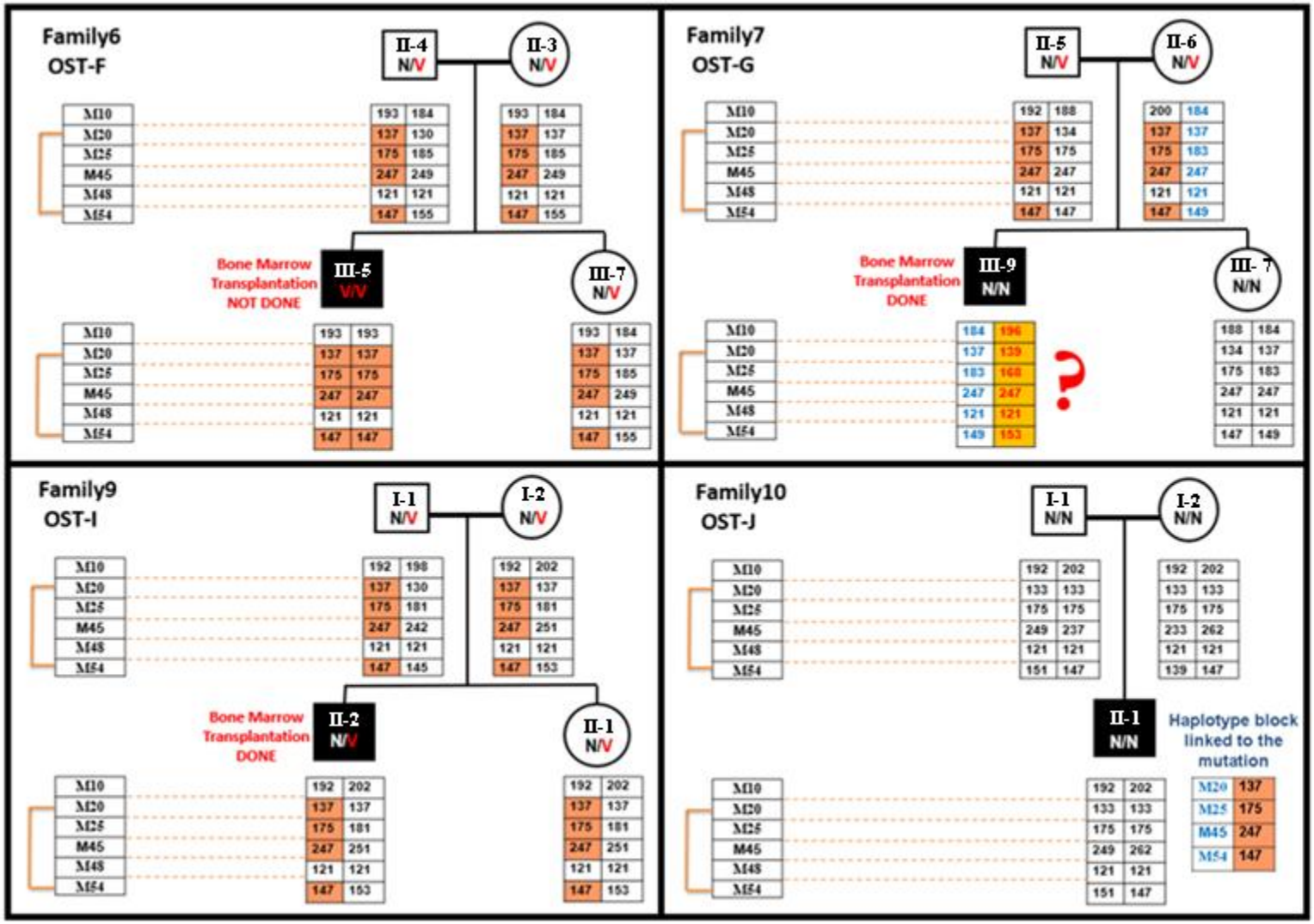

Figure 24: Haplotype analysis results for Families 6, 7, 9 and 10 (OST-J Family was used as a negative control), also the minimum haplotype block is shown in the figure. Different colors mean different haplotypes while the same color indicates the same haplotype.

5.3. Clinical Assessment and Pedigree of Family 10

Family 10 individuals were recruited from Shibteen village in the west of Ramallah and a comprehensive oral exam was conducted on family members for pedigree construction, as indicated in Figure 25: Family 10 (OST-J). One four months old male child (J/II-1) of a first-cousin marriage, were referred to us for genetic diagnosis with a clinical picture of ARO. Patient J/II-1 was admitted to the pediatric hematology service at Hadassah hospital for evaluation for bone marrow transplantation (BMT).

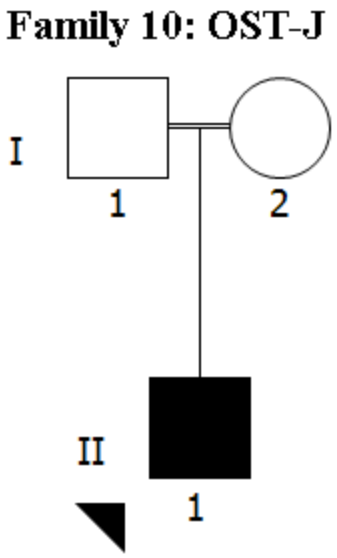

Figure 25: Pedigree of family 1 (OST-A) with Malignant Infantile Osteopetrosis, showing affection status of sampled individuals.

5.3.1. Whole-Exome Sequencing Analysis Results in Family 10

Individual J/II-1 underwent whole-exome sequencing. Variants were filtered by selecting nonsense, splice-site, coding indel variants and nonsynymous variants with PolyPhen2 > 0.5 / unknown and with a minor allele frequency of less than 0.001% in ExAC browser. Potentially deleterious allele/alleles that met the filtering criteria and fit the phenotype were tested for

segregation in Family 10. A homozygous nonframshift variant in *TCIRG1* gene (*TCIRG1*_p.N462del) at chr11: 67,815,190- chr11: 67,815,192 (according to GRCh37/hg19 assembly) was identified in J/II-1 patient.

5.3.2. Family Segregation Analysis for *TCIRG1*_p.N462del Variant Gene in Family10

The target gDNA position and flanking sequences were amplified in all available family members using the primers listed in Appendix I (Table 7). The PCR products were then sequenced in both directions (Figure 26). Segregation analysis confirmed that the *TCIRG1*_p.N462del variant was present in the affected individual. Unaffected parents were carriers for this variant (Figure 27).

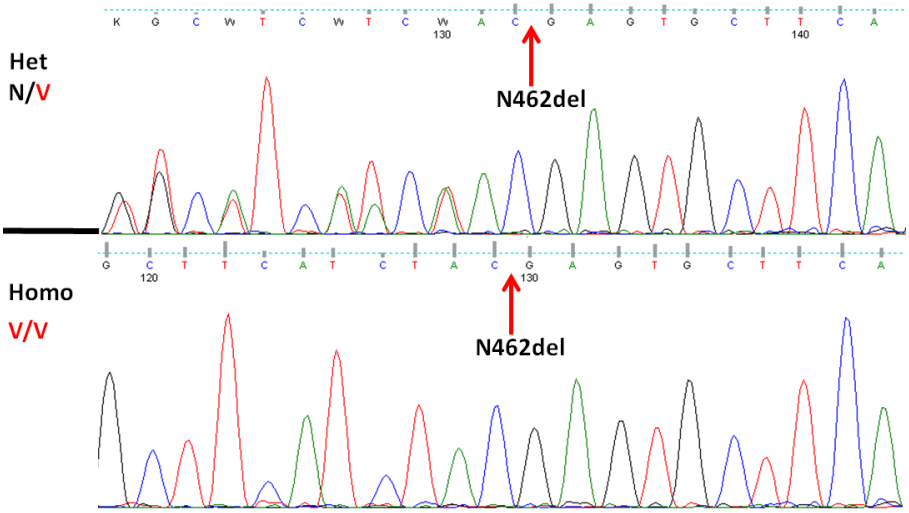

Figure 26: Sanger sequencing results of *TCIRG1* gene in family 10; Individual J/II-1 is homozygous for p.N462del, while parents J/I-1 and J/I-2 are heterozygous for the mutation.

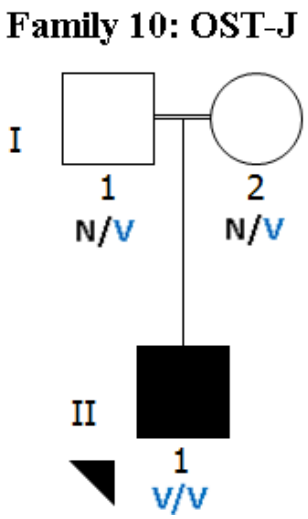

Figure 27: Pedigree of family 10 displaying TCIRG1_p.N462del genotype of sampled individuals.

CHAPTER 6

Discussion

In this thesis, we report deleterious mutations that are responsible for the development of ARO in 10 Palestinian families. Unfortunately, whole exome sequencing for family 1 (OST-A) could not identify any homozygous or compound heterozygous pathogenic, disease-related variants. This can be explained in several ways. First, the variant might be outside the coding region or in deep intronic regions or in trans-regulatory regions not covered by WES. Second, the cause of the phenotype might be due to small duplications/deletions not captured by WES. Third, the cause of the phenotype might be in undiscovered genes or in genes of undiscovered function yet, therefore, data re-analysis is recommended in few months.

Whole exome sequencing of family7 (OST-G) affected individuals identified a missense mutation in *SNX10* gene causing an amino acid replacement in a highly conserved residue, R51Q (Aker et al., 2012). Sanger sequencing confirmed that *SNX10*_p.R51Q is the causative variant also in families 2, 3, 4, 5, 6, and 9. Referring to the literature, this mutation has been found in many families of Palestinian origin due to the high degree of consanguinity (Aker et al., 2012). Even though, Family 8 (OST-H) belongs to the same clan of other Al-Karma families, it doesn't have any mutation in SNX10 gene which was confirmed by direct sequencing of exonic regions of this gene. Thus, it remains a good candidate family for whole exome sequencing test is the near future.

Moreover, microsatellite analysis results revealed that the shared haplotype block in these families reflects sharing a common ancestry. And having different haplotype block in the control family 10 (OST-J) which has different disease gene mutation gives an additional evidence and

confirm that this haplotype block is linked to p.R51Q mutation, and exclude the possibility of sharing it by pure chance in an endogamous population. The shared haplotype block also suggests that the spread of the p.R51Q mutation among Al-Karma patients have been influenced by a common founder effect in these Palestinian families. Also, this indicates that the p.R51Q mutation represents a frequently occurring mutation in a hot spot mutation region. This has also encouraged us to do p.R51Q mutation screening in Al-Karma village to identify the carrier frequency and increase awareness of the risks associated with consanguineous marriages.

Additionally, the establishment of genetic linkage between a tagging SNP such as the p.R51Q and a distinct haplotype block (STR) provide a very useful diagnostic tool for preimplantation genetic diagnosis (PGD) purpose, which requires absolute certainty of the existence of the disease allele. Because direct mutational analysis of a missense mutation such as *SNX10*_p.R51Q genotype may not be feasible on a single blastomere level and could easily lead to misdiagnosis and the inability of elimination of homozygous affected embryos. The establishment of haplotypes for genetically informative markers linked to the locus of the disease gene can really help in the correct assignment of embryos genotypes and the decision of whether or not to accept an embryo for transfer.

SNX10 protein as previously indicated participates in the regulation of endosome sorting in cells. SNX10 protein contain a phospholipid-binding motif (the PX domain), which mediates the ability to interact with cellular membrane compartments for protein sorting and membrane trafficking purposes (Teasdale et al., 2012). Our mutation p.R51Q is located in this PX domain, and thus, not surprisingly, it hinders the ability of SNX10 protein to interact with other proteins or membrane compartments. In fact, it was shown that SNX10 associates with the ATP-

dependent vacuolar proton pump of osteoclast cells (V-ATPase) and aids in its localization to the ruffled border of these osteoclasts (Palagano et al., 2018; Pangrazio et al., 2013). Thus, p.R51Q mutation in *SNX10* would therefore result in an indirect V-ATPase deficiency, inability to acidify the resorption lacuna, and osteoclast function failure, which explains osteopetrosis phenotype in Al-Karma families. It is currently estimated that mutations in SNX10 account for 5% of ARO cases globally (Palagano et al., 2018; Pangrazio et al., 2013; Stattin et al., 2017).

Here we also report a homozygous nonframshift variant p.Asn462del in *TCIRG1* gene in family 10 (OST-J) revealed by Whole exome sequencing for J/II-1. The p.N462del variant alters a highly conserved residue which lies within the transmembrane region of TCIRG1 protein. As mentioned earlier, *TCIRG1* gene encodes the 'a3' subunit of the vacuolar proton pump (V-ATPase), which mediates the acidification of the bone/osteoclast interface. The inactivation of this acidification function results in an imbalance of the bone remodeling process, leading to an osteopetrotic phenotype. Mutations in *TCIRG1* gene are responsible for more than one-half of the ARO patients.

Like an orchestra, cellular components of bone work together in a highly cooperative and coordinated way. Bone formation by osteoblasts and bone and resorption by osteoclasts are in balance resulting in no net change in bone mass and strength. These two activities are tightly coupled in a process known as bone remodeling (Sims and Gooi, 2008). To maintain bone homeostasis, many factors regulate the intercellular communication between osteoblasts and osteoclasts. For example, differentiated osteoblasts controls osteoclast differentiation by major signaling factors produced by osteoblast lineage cells such as OPG and RANKL (Simonet et al., 1997). On the other hand, osteoclasts can control osteoblast chemotaxis via osteoclast-produced

growth factors and provides a mechanism by which bone rebuilding and repair can occur (Sanchez-Fernandez et al., 2008). Therefore, any alteration in coupling mechanism between bone resorption and formation results in several pathological conditions. Genetic mutations that cause osteopetrosis may have different cellular consequences and different Osteoclast/Osteoblast profile depending on the nature of the mutant genes and the mutation site. ARO mutations may result in a normal/decreased number of non-functional osteoclasts or increased number of non-resorbing osteoclasts. ARO caused by homozygous or compound heterozygous mutations in TCIRG1 gene results in ablated osteoclast function, but not number (Del Fattore et al., 2006; Sobacchi et al., 2013). The main cellular phenotype in patients with mutations in TCIRG1 is the higher amount of non-resorbing osteoclasts found in bone biopsies compared to osteoclasts in healthy individuals and is therefore referred to as an osteoclast-rich osteopetrosis (Flanagan et al., 2000; Frattini et al., 2000; Taranta et al., 2003). Mutations in SNX10 gene affect both the number and functionality of osteoclast cells. The scarcity of osteoclasts in homozygous mutations in SNX10 gene is caused by deregulated fusion that results in formation of giant, unstable osteoclast cells (Barnea et al., 2018). The altered morphology and the lack of ruffled borders of the mature osteoclasts explain their disrupted resorptive activity (Barnea et al., 2018).

On the molecular level, both scenarios of *TCIRG1*-dependent ARO or *SNX10*-dependent ARO will lead to V-ATPase deficiency weather directly or indirectly as we have already discussed. And mutations in these two genes will lead to almost the same phenotype of impaired extracellular acidification capacity of osteoclasts and bone resorption failure.

CHAPTER 7

Conclusion

Despite the major advances in understanding of osteopetrosis pathogenesis, the elucidation of the molecular genetic basis remains to be undefined in approximately 30% of cases.

In this study we succeeded in solving the genetic basis of eight Palestinian osteopetrosis families out of ten studied families. Genetic testing has revealed two pathogenic mutations in important genes; *SNX10, and TCIRG1* which are involved in maintaining an acidic environment at the bone-osteoclast interface necessary for osteoclastic bone resorption function. These results confirm the contribution of SNX10 protein in osteoclast physiology and confirm the involvement of SNX10 gene mutations in ARO, because until now the pathogenic contribution of SNX10 gene in osteopetrosis disease is not confirmed with certainty. On the other hand, TCIRG*1* gene role in osteoclast function is massively studied, as two-thirds of osteopetrosis cases are caused by mutations in *TCIRG1* gene, but our findings enrich the database of *TCIRG1* mutations.

Generally, patients with mutant *SNX10* or *TCIRG1* experience life-threatening symptoms including anemia, pancytopenia, and impaired medullary hematopoiesis, associated with secondary hematopoiesis in liver and spleen that causes hepatosplenomegaly. Bone marrow transplantation (BMT) represents the only curative therapy at the present time. However, haemopoietic potential is restored by BMT only if the surgery is done very early on of their lives, and it can be curative when the donor is HLA-identical with almost an 80% 5-year progression-free survival. However, functional impairments of the skeletal system and dental and vision problems rarely significantly improves even after successful BMT.

Finally, Genetic testing has made it possible to establish as early and accurate diagnoses of osteopetrosis cases. Moreover, genetic counseling help in reducing the incidence of osteopetrosis cases by doing genetic carrier screening tests to identify heterozygote carriers of pathogenic mutations in important osteopetrosis genes. Mutation carriers of different related families reside in the same region and should be aware of their genetic status before stepping into marriages especially when consanguineous marriages are opted for. Moreover, preconception genetic screening prior to pregnancy onset, when the family has a known history of recessive genetic disorders, help in reducing the incidence of birth defects. Moreover, the transmission of the mutated gene from both parents to their offspring can be prevented by doing IVF-PGD/PGS to increase the chances of transferring a healthy embryo.

CHAPTER 8

References

Aker, M., Rouvinski, A., Hashavia, S., Ta-Shma, A., Shaag, A., Zenvirt, S., ... & Elpeleg, O. (2012). An SNX10 mutation causes malignant osteopetrosis of infancy. *Journal of medical genetics*, *49*(4), 221-226.

Askmyr, M., Flores, C., Fasth, A., & Richter, J. (2009). Prospects for gene therapy of osteopetrosis. *Current gene therapy*, *9*(3), 150-159.

Aubin, J. E. (2001). Regulation of osteoblast formation and function. *Reviews in Endocrine and Metabolic Disorders*, *2*(1), 81-94.

Balemans, W., Van Wesenbeeck, L., & Van Hul, W. (2005). A clinical and molecular overview of the human osteopetroses. *Calcified tissue international*, *77*(5), 263-274.

Ballet, J. J., Griscelli, C., Coutris, C., Milhaud, G., & Maroteaux, P. (1977). Bone-marrow transplantation in osteopetrosis. *The Lancet*, *310*(8048), 1137.

Barnea, M., Stein, M., Winograd-Katz, S., Shalev, M., Arman, E., Brenner, O., ... & Geiger, B. (2018). R51Q SNX10 induces osteopetrosis by promoting uncontrolled fusion of monocytes to form giant, non-functional osteoclasts. *bioRxiv*, 332551.

Baron, R. (1989). Molecular mechanisms of bone resorption by the osteoclast. *The Anatomical Record*, *224*(2), 317-324.

Blazer, D. G., & Hernandez, L. M. (Eds.). (2006). *Genes, behavior, and the social environment: Moving beyond the nature/nurture debate*. National Academies Press.

Bollerslev, J., Marks Jr, S. C., Pockwinse, S., Kassem, M., Brixen, K., Steiniche, T., & Mosekilde, L. (1993). Ultrastructural investigations of bone resorptive cells in two types of autosomal dominant osteopetrosis. *Bone*, *14*(6), 865-869.

Bonewald, L. F. (2011). The amazing osteocyte. *Journal of bone and mineral research*, *26*(2), 229-238.

Boyle, W. J., Simonet, W. S., & Lacey, D. L. (2003). Osteoclast differentiation and activation. *Nature*, *423*(6937), 337.

Campos-Xavier, A., Saraiva, J. M., Ribeiro, L. M., Munnich, A., & Cormier-Daire, V. (2003). Chloride channel 7 (CLCN7) gene mutations in intermediate autosomal recessive osteopetrosis. *Human genetics*, *112*(2), 186-189.

Capulli, M., Paone, R., & Rucci, N. (2014). Osteoblast and osteocyte: games without frontiers. *Archives of biochemistry and biophysics*, *561*, 3-12.

Chalhoub, N., Benachenhou, N., Rajapurohitam, V., Pata, M., Ferron, M., Frattini, A., ... & Vacher, J. (2003). Grey-lethal mutation induces severe malignant autosomal recessive osteopetrosis in mouse and human. *Nature medicine*, *9*(4), 399.

Chen, Y., Wu, B., Xu, L., Li, H., Xia, J., Yin, W., ... & Shu, X. (2012). A SNX10/V-ATPase pathway regulates ciliogenesis in vitro and in vivo. *Cell research*, *22*(2), 333.

Clarke, B. (2008). Normal bone anatomy and physiology. *Clinical journal of the American Society of Nephrology*, *3*(Supplement 3), S131-S139.

Cleiren, E., Bénichou, O., Van Hul, E., Gram, J., Bollerslev, J., Singer, F. R., ... & deVernejoul, M. C. (2001). Albers-Schönberg disease (autosomal dominant osteopetrosis, type II) results from mutations in the ClCN7 chloride channel gene. *Human molecular genetics*, *10*(25), 2861-2867.

Coccia, P. F., Krivit, W., Cervenka, J., Clawson, C., Kersey, J. H., Kim, T. H., ... & Kahn, A. J. (1980). Successful bone-marrow transplantation for infantile malignant osteopetrosis. *New England Journal of Medicine*, *302*(13), 701-708.

Cummings, T. J., & Proia, A. D. (2004). Optic nerve compression in infantile malignant autosomal recessive osteopetrosis. *Journal of pediatric ophthalmology and strabismus*, *41*(4), 241-244.

Del Fattore, A., Cappariello, A., & Teti, A. (2008). Genetics, pathogenesis and complications of osteopetrosis. *Bone*, *42*(1), 19-29.

Del Fattore, A., Peruzzi, B., Rucci, N., Recchia, I., Cappariello, A., Longo, M., ... & Devito, R. (2006). Clinical, genetic, and cellular analysis of 49 osteopetrotic patients: implications for diagnosis and treatment. *Journal of medical genetics*, *43*(4), 315-325.

Dole, N. S. (2015). Genetic Determinants of Skeletal Diseases: Role of microRNAs.

Driessen, G. J. A., Gerritsen, E. J. A., Fischer, A., Fasth, A., Hop, W. C. J., Veys, P., ... & Uckan, D. (2003). Long-term outcome of haematopoietic stem cell transplantation in autosomal recessive osteopetrosis: an EBMT report. *Bone marrow transplantation*, *32*(7), 657.

Fasth, A., & Porras, O. (1999). Human malignant osteopetrosis: pathophysiology, management and the role of bone marrow transplantation. *Pediatric transplantation*, *3*, 102-107.

Felix, R., Cecchini, M. G., & Fleisch, H. (1990). Macrophage colony stimulating factor restores in vivo bone resorption in the op/op osteopetrotic mouse. *Endocrinology*, *127*(5), 2592-2594.

Franceschetti, T., Dole, N. S., Kessler, C. B., Lee, S. K., & Delany, A. M. (2014). Pathway analysis of microRNA expression profile during murine osteoclastogenesis. *PloS one*, *9*(9), e107262.

Frattini, A., Pangrazio, A., Susani, L., Sobacchi, C., Mirolo, M., Abinun, M., ... & Notarangelo, L. D. (2003). Chloride channel ClCN7 mutations are responsible for severe recessive, dominant, and intermediate osteopetrosis. *Journal of bone and mineral research*, *18*(10), 1740-1747.

Frattini, A., Orchard, P. J., Sobacchi, C., Giliani, S., Abinun, M., Mattsson, J. P., ... & Notarangelo, L. D. (2000). Defects in TCIRG1 subunit of the vacuolar proton pump are responsible for a subset of human autosomal recessive osteopetrosis. *Nature genetics*, *25*(3), 343.

Froeschke, G., & von der Heyden, S. (2014). A review of molecular approaches for investigating patterns of coevolution in marine host–parasite relationships. In *Advances in parasitology* (Vol. 84, pp. 209-252). Academic Press.

Gerritsen, E. J., Vossen, J. M., Fasth, A., Friedrich, W., Morgan, G., Padmos, A., ... & Bordigoni, P. (1994). Bone marrow transplantation for autosomal recessive osteopetrosis A report from the Working Party on Inborn Errors of the European Bone Marrow Transplantation Group. *The Journal of pediatrics*, *125*(6), 896-902.

Guerrini, M. M., Sobacchi, C., Cassani, B., Abinun, M., Kilic, S. S., Pangrazio, A., ... & Coxon, F. P. (2008). Human osteoclast-poor osteopetrosis with hypogammaglobulinemia due to TNFRSF11A (RANK) mutations. *The American Journal of Human Genetics*, *83*(1), 64-76.

Henriksen, K., Gram, J., Høegh-Andersen, P., Jemtland, R., Ueland, T., Dziegiel, M. H., ... & Karsdal, M. A. (2005). Osteoclasts from patients with autosomal dominant osteopetrosis type I caused by a T253I mutation in low-density lipoprotein receptor-related protein 5 are normal in vitro, but have decreased resorption capacity in vivo. *The American journal of pathology*, *167*(5), 1341-1348.

Herman, T. E., & Siegel, M. J. (2007). Infantile autosomal-recessive malignant osteopetrosis. *Journal of Perinatology*, *27*(7), 455.

Hollberg, K., Hultenby, K., Hayman, A. R., Cox, T. M., & Andersson, G. (2002). Osteoclasts from mice deficient in tartrate-resistant acid phosphatase have altered ruffled borders and disturbed intracellular vesicular transport. *Experimental cell research*, *279*(2), 227-238.

Jefferies, K. C., Cipriano, D. J., & Forgac, M. (2008). Function, structure and regulation of the vacuolar (H+)-ATPases. *Archives of biochemistry and biophysics*, *476*(1), 33-42.

Kornak, U., Schulz, A., Friedrich, W., Uhlhaas, S., Kremens, B., Voit, T., ... & Kubisch, C. (2000). Mutations in the a3 subunit of the vacuolar H+-ATPase cause infantile malignant osteopetrosis. *Human molecular genetics*, *9*(13), 2059-2063.

Kornak, U., Kasper, D., Bösl, M. R., Kaiser, E., Schweizer, M., Schulz, A., ... & Jentsch, T. J. (2001). Loss of the ClC-7 chloride channel leads to osteopetrosis in mice and man. *Cell*, *104*(2), 205-215.

Lazner, F., Gowen, M., Pavasovic, D., & Kola, I. (1999). Osteopetrosis and osteoporosis: two sides of the same coin. *Human molecular genetics*, *8*(10), 1839-1846.

Lézot, F., Chesneau, J., Navet, B., Gobin, B., Amiaud, J., Choi, Y., ... & Rédini, F. (2015). Skeletal consequences of RANKL-blocking antibody (IK22-5) injections during growth: Mouse strain disparities and synergic effect with zoledronic acid. *Bone*, *73*, 51-59.

Li, J., Sarosi, I., Yan, X. Q., Morony, S., Capparelli, C., Tan, H. L., ... & Kaufman, S. (2000). RANK is the intrinsic hematopoietic cell surface receptor that controls osteoclastogenesis and regulation of bone mass and calcium metabolism. *Proceedings of the National Academy of Sciences*, *97*(4), 1566-1571.

Li, Y. P., Chen, W., Liang, Y., Li, E., & Stashenko, P. (1999). Atp6i-deficient mice exhibit severe osteopetrosis due to loss of osteoclast-mediated extracellular acidification. *Nature genetics*, *23*(4), 447.

Long, F., & Ornitz, D. M. (2013). Development of the endochondral skeleton. *Cold Spring Harbor perspectives in biology*, *5*(1), a008334.

Makaryan, V., Rosenthal, E. A., Bolyard, A. A., Kelley, M. L., Below, J. E., Bamshad, M. J., ... & Skokowa, J. (2014). TCIRG1- associated congenital neutropenia. *Human mutation*, *35*(7), 824-827.

Manolagas, S. C. (2000). Birth and death of bone cells: basic regulatory mechanisms and implications for the pathogenesis and treatment of osteoporosis. *Endocrine reviews*, *21*(2), 115-137.

Margolis, D. S., Szivek, J. A., Lai, L. W., & Lien, Y. H. H. (2008). Phenotypic characteristics of bone in carbonic anhydrase II-deficient mice. *Calcified tissue international*, *82*(1), 66-76.

Marks Jr, S. C., Seifert, M. F., & Lane, P. W. (1985). Osteosclerosis, a recessive skeletal mutation on chromosome 19 in the mouse. *Journal of Heredity*, *76*(3), 171-176.

Marín-García, J. (2011). *Post-genomic cardiology*. Academic Press.

Martin, T. J., & Seeman, E. (2008). Bone remodelling: its local regulation and the emergence of bone fragility. *Best practice & research Clinical endocrinology & metabolism*, *22*(5), 701-722.

MCDONALD, D. B., & POTTS, W. K. (1997). DNA microsatellites as genetic markers at several scales. In *Avian molecular evolution and systematics* (pp. 29-49). Academic Press.

Mégarbané, A., Pangrazio, A., Villa, A., Chouery, E., Maarawi, J., Sabbagh, S., ... & Sobacchi, C. (2013). Homozygous stop mutation in the SNX10 gene in a consanguineous Iraqi boy with osteopetrosis and corpus callosum hypoplasia. *European journal of medical genetics*, *56*(1), 32-35.

Palagano, E., Menale, C., Sobacchi, C., & Villa, A. (2018). Genetics of osteopetrosis. *Current osteoporosis reports*, *16*(1), 13-25.

Pettit, A. R., Ji, H., von Stechow, D., Müller, R., Goldring, S. R., Choi, Y., ... & Gravallese, E. M. (2001). TRANCE/RANKL knockout mice are protected from bone erosion in a serum transfer model of arthritis. *The American journal of pathology*, *159*(5), 1689-1699.

Popoff, S. N., & Marks Jr, S. C. (1995). The heterogeneity of the osteopetroses reflects the diversity of cellular influences during skeletal development. *Bone*, *17*(5), 437-445.

Sanchez-Fernandez, M. A., Gallois, A., Riedl, T., Jurdic, P., & Hoflack, B. (2008). Osteoclasts control osteoblast chemotaxis via PDGF-BB/PDGF receptor beta signaling. *PloS one*, *3*(10), e3537.

Seeman, E., & Delmas, P. D. (2006). Bone quality—the material and structural basis of bone strength and fragility. *New England journal of medicine*, *354*(21), 2250-2261.

Shalhoub, V., Elliott, G., Chiu, L., Manoukian, R., Kelley, M., Hawkins, N., ... & Van, G. (2000). Characterization of osteoclast precursors in human blood. *British journal of haematology*, *111*(2), 501-512.

Simonet, W. S., Lacey, D. L., Dunstan, C. R., Kelley, M. C. M. S., Chang, M. S., Lüthy, R., ... & Shimamoto, G. (1997). Osteoprotegerin: a novel secreted protein involved in the regulation of bone density. *Cell*, *89*(2), 309-319.

Sims, N. A., & Gooi, J. H. (2008, October). Bone remodeling: Multiple cellular interactions required for coupling of bone formation and resorption. In *Seminars in cell & developmental biology* (Vol. 19, No. 5, pp. 444-451). Academic Press.

Sims, N. A., & Vrahnas, C. (2014). Regulation of cortical and trabecular bone mass by communication between osteoblasts, osteocytes and osteoclasts. *Archives of biochemistry and biophysics*, *561*, 22-28.

Sobacchi, C., Frattini, A., Guerrini, M. M., Abinun, M., Pangrazio, A., Susani, L., ... & Grabowski, P. (2007). Osteoclast-poor human osteopetrosis due to mutations in the gene encoding RANKL. *Nature genetics*, *39*(8), 960.

Sobacchi, C., Frattini, A., Orchard, P., Porras, O., Tezcan, I., Andolina, M., ... & Dupuis-Girod, S. (2001). The mutational spectrum of human malignant autosomal recessive osteopetrosis. *Human molecular genetics*, *10*(17), 1767-1773.

Sobacchi, C., Schulz, A., Coxon, F. P., Villa, A., & Helfrich, M. H. (2013). Osteopetrosis: genetics, treatment and new insights into osteoclast function. *Nature Reviews Endocrinology*, *9*(9), 522.

Sun-Wada, G. H., & Wada, Y. (2015). Role of vacuolar-type proton ATPase in signal transduction. *Biochimica et Biophysica Acta (BBA)-Bioenergetics*, *1847*(10), 1166-1172.

Sun-Wada, G. H., & Wada, Y. (2013). Vacuolar-type proton pump ATPases: acidification and pathological relationships. *Histology and histopathology*, *28*(7), 805-815.

Stevens, T. H., & Forgac, M. (1997). Structure, function and regulation of the vacuolar (H+)-ATPase. *Annual review of cell and developmental biology*, *13*(1), 779-808.

Taranta, A., Migliaccio, S., Recchia, I., Caniglia, M., Luciani, M., De Rossi, G., ... & Lanino, E. (2003). Genotype-phenotype relationship in human ATP6i-dependent autosomal recessive osteopetrosis. *The American journal of pathology*, *162*(1), 57-68.

Tavares, B., Vaz, A., Pintado, P., & Lopes, S. S. (2012). Investigation of a new signalling pathway linking deltaD to ciliogenesis-the role of rabconnectin3. *Cilia*, *1*(S1), P50.

Teasdale, R. D., & Collins, B. M. (2012). Insights into the PX (phox-homology) domain and SNX (sorting nexin) protein families: structures, functions and roles in disease. *Biochemical Journal*, *441*(1), 39-59.

Teitelbaum, S. L. (2000). Bone resorption by osteoclasts. *Science*, *289*(5484), 1504-1508.

Teitelbaum, S. L. (2007). Osteoclasts: what do they do and how do they do it?. *The American journal of pathology*, *170*(2), 427-435.

Tolar, J., Teitelbaum, S. L., & Orchard, P. J. (2004). Osteopetrosis. *New England Journal of Medicine*, *351*(27), 2839-2849.

Toyomura, T., Oka, T., Yamaguchi, C., Wada, Y., & Futai, M. (2000). Three Subunit a Isoforms of Mouse Vacuolar H+-ATPase PREFERENTIAL EXPRESSION OF THE a3 ISOFORM DURING OSTEOCLAST DIFFERENTIATION. *Journal of Biological Chemistry*, *275*(12), 8760-8765.

Väänänen, H. K., & Horton, M. (1995). The osteoclast clear zone is a specialized cell-extracellular matrix adhesion structure. *Journal of cell science*, *108*(8), 2729-2732.

Vernejoul, M. C., & B nichou, O. (2001). Human osteopetrosis and other sclerosing disorders: recent genetic developments. *Calcified Tissue International*, *69*(1), 1-6.

Waguespack, S. G., Hui, S. L., DiMeglio, L. A., & Econs, M. J. (2007). Autosomal dominant osteopetrosis: clinical severity and natural history of 94 subjects with a chloride channel 7 gene mutation. *The Journal of Clinical Endocrinology & Metabolism*, *92*(3), 771-778.

Walker, D. G. (1975a). Bone resorption restored in osteopetrotic mice by transplants of normal bone marrow and spleen cells. *Science*, *190*(4216), 784-785.

Walker, D. G. (1975b). Control of bone resorption by hematopoietic tissue. The induction and reversal of congenital osteopetrosis in mice through use of bone marrow and splenic transplants. *Journal of Experimental Medicine*, *142*(3), 651-663.

Wang, Q., & Seeman, E. (2013). Skeletal growth and peak bone strength. *Primer on the Metabolic Bone Diseases and Disorders of Mineral Metabolism*, 127-134.

Way, K. J., Dinh, H., Keene, M. R., White, K. E., Clanchy, F. I., Lusby, P., ... & Hamilton, J. A. (2009). The generation and properties of human macrophage populations from hemopoietic stem cells. *Journal of leukocyte biology*, *85*(5), 766-778.

Wilson, C. J., & Vellodi, A. (2000). Autosomal recessive osteopetrosis: diagnosis, management, and outcome. *Archives of disease in childhood*, *83*(5), 449-452.

Yagi, M., Miyamoto, T., Sawatani, Y., Iwamoto, K., Hosogane, N., Fujita, N., ... & Oike, Y. (2005). DC-STAMP is essential for cell–cell fusion in osteoclasts and foreign body giant cells. *Journal of Experimental Medicine*, *202*(3), 345-351.

Yang, Y., Muzny, D. M., Reid, J. G., Bainbridge, M. N., Willis, A., Ward, P. A., ... & Hardison, M. (2013). Clinical whole-exome sequencing for the diagnosis of mendelian disorders. *New England Journal of Medicine*, *369*(16), 1502-1511.

Yao, D., Wu, B., Qin, B., & Pei, D. (2009). PX domain and CD domain play different roles in localization and vacuolation of Sorting Nexin 10. *Chinese Science Bulletin*, *54*(21), 3965.

Young, P. R., & Vivier, M. A. (2010). Genetics and genomic approaches to improve grape quality for winemaking. In *Managing wine quality* (pp. 316-364). Woodhead Publishing.

Zhao, Q., Shao, J., Chen, W., & Li, Y. P. (2007). Osteoclast differentiation and gene regulation. *Front Biosci*, *12*(1), 2519-2529.

Zlotogora, J. (1997). Autosomal recessive diseases among Palestinian Arabs. *Journal of medical genetics*, *34*(9), 765-766.

Zou, W., Kitaura, H., Reeve, J., Long, F., Tybulewicz, V. L., Shattil, S. J., ... & Teitelbaum, S. L. (2007). Syk, c-Src, the αvβ3 integrin, and ITAM immunoreceptors, in concert, regulate osteoclastic bone resorption. *The Journal of cell biology*, *176*(6), 877-888.

CHAPTER 9

Appendix I: Primer Sequences

Table 7. Primer sequences used for validation and Sanger sequencing.

Primer Name	Sequence
Primers used for Sanger sequencing in Family 1	
*CLCN7*_p.G521R	**Forward:** 5' CACTTTTGTCCTGCCCTGG 3' **Reverse:** 5' CTGTGAGGCCCGAGACTG 3'
*ADCY6*_p.I1106M	**Forward:** 5' CACAGAACACTAGCCACCCT 3' **Reverse:** 5' TGCTGTTCTCTCCACCTCAG 3'
*KRT82*_p.Y315X	**Forward:** 5' TGGCACTCACAGCAAGGATT 3' **Reverse:** 5' AGGACCCAAAATTGCCCAGA 3'
*PMEL*_p.R192Q	**Forward:** 5' GCACAGCATTTCACCTTTCTCC 3' **Reverse:** 5' TCCTGACCTCCCATCTCCAG 3'
*GNAS*_ p.E357Q	**Forward:** 5' GTTCGAGATTGGCAGCGC 3' **Reverse:** 5' GTCGGGATCTTCTGGGGTTG 3'
*ERCC2*_c.-325T>C	**Forward:** 5' TCTCCTCGCTATCACTGCTG 3' **Reverse:** 5' AATATAGGTGGAGCGAGCCC 3'
Primers used for *SNX10*_p.R51Q in Family 2, 3, 4, 5, 6, 7, 8, 9	
*SNX10*_p.R51Q	**Forward:** 5' TCCTGGGTTATGTGCAAGATT 3' **Reverse:** 5' CACTTACACCAGCAACGCAT 3'
Primers used for *TCIRG1*_p.N462del in Family 10	
*TCIRG1*_p.N462del	**Forward:** 5' ATGAGGGTAGCAGGGCCA 3' **Reverse:** 5' GGGATCCAGGGTAAGCATCG 3'
Primers used for STR Markers of SNX10 gene in Family2, 3, 4, 5, 6, 7, 9, 10 (The blue sequence attached to the forward primer is the FAM tail)	
M10 (22xTG)	**Forward:** 5'gtgcagagcatcatgcCATAGGGCTTTGTTGTTTAGCATCC 3' **Reverse:** 5' ATCCTGTCCAATTAACTGCCTCAAG 3'
M20 (20xTG)	**Forward:** 5'gtgcagagcatcatgcGTCTGGGAGTCGATATACCTTCAAG 3' **Reverse:** 5' TATGTTTCCTATTCATGCCTCCACT 3'
M25 (20xAC)	**Forward:** 5' gtgcagagcatcatgcCAGCACTCACAGCCACCACTTTCAC 3' **Reverse:** 5' ATGTATGATTGACAGCAGGGAGAG 3'
M45 (24xGT)	**Forward:** 5' gtgcagagcatcatgcGAACTCAGAACAGAGAAGCGGGAAC 3' **Reverse:** 5' TGTTTCAAACACAGAAATACAGAGGA 3'
M48 (22xGT)	**Forward:** 5' gtgcagagcatcatgcAAGAGGTTATGAGTGGCAAAGTTCA 3' **Reverse:** 5' AGATCTAATCATGCCCTCTGGATTC 3'
M54 (24xAC)	**Forward:** 5' gtgcagagcatcatgcTCTCCGTAATTGCTTTAGCCAATTC 3' **Reverse:** 5' CTCCAGATAAATAGAACCAACAGGG 3'